Journal
of
The Franklin Institute

EDITOR, HENRY BUTLER ALLEN, MET.E., D.Sc., Sc.D.
EDITORIAL ASSISTANT, NANCY S. GLENN, M.A.

Associate Editors:

WILDER D. BANCROFT, PH.D.
C. B. BAZZONI, PH.D.
ARTHUR L. DAY, SC.D.
R. KESERGIAN, PH.D.
PAUL D. FOOTE, PH.D.
W. J. HUMPHREYS, PH.D.
C. E. K. MEES, D.SC.
WILLIAM B. MELDRUM, PH.D.
HENRY C. SHERMAN, SC.D.
W. F. G. SWANN, D.SC.
HUGH S. TAYLOR, D.SC.
A. F. ZAHM, PH.D.
JOHN ZELENY, PH.D.

Committee on Publications:

G. H. CLAMER, CHAIRMAN
RICHARD HOWSON
C. L. JORDAN
LIONEL F. LEVY
HIRAM S. LUKENS
RICHARD H. OPPERMANN
WINTHROP R. WRIGHT

Vol. 248 **SEPTEMBER, 1949** **No. 3**

CONTENTS

Development, Design and Construction of Electrical Condensers. WILLIAM DUBILIER 193
Energy Fluctuations in a Van der Pol Oscillator. . . . . N. MINORSKY 205
Minimum and Maximum Sensitivities of Photographic Emulsions. . A. P. H. TRIVELLI 225
Stress-Strain Relations in the Plastic Range for Biaxial Stresses. . . . . JOSEPH MARIN 231
Preparation of Vanadium Pentoxide Sols by Ion Exchange
JAMES A. DEVLIN, WALLACE M. MCNABB AND FRED HAZEL 251
Notes from the National Bureau of Standards. 254
The Franklin Institute
The Franklin Institute Laboratories for Research and Development. 256
Journal of The Franklin Institute. 258
Bartol Research Foundation. 258
Library. 260
Museum. 261
Notes from the Biochemical Research Foundation. 263
Absorption of Ultra-Violet Light by Living Cells. . . . . J. O. ELY AND M. H. ROSS
Book Reviews. 265
Book Notes. 268
Current Topics. 224, 230, 250, 270

Published at
Prince and Lemon Streets, Lancaster, Penna., by
THE FRANKLIN INSTITUTE OF THE STATE OF PENNSYLVANIA
Benjamin Franklin Parkway at Twentieth St., Philadelphia 3, Penna.

DOMESTIC—EIGHT DOLLARS PER YEAR **FOREIGN—NINE DOLLARS PER YEAR**
(Foreign Postage Additional)
SINGLE CURRENT NUMBERS—ONE DOLLAR EACH
REPRINTS—FIFTY CENTS PER INDIVIDUAL INSTALLMENTS

Indexes to the semi-annual volumes of the JOURNAL
are published with the June and December numbers

Journal
of
The Franklin Institute
Devoted to Science and the Mechanic Arts

Vol. 248 SEPTEMBER, 1949 No. 3

DEVELOPMENT, DESIGN AND CONSTRUCTION OF ELECTRICAL CONDENSERS *

BY

WILLIAM DUBILIER [1]

Any electrical apparatus, however complex, is composed, essentially, of one or more devices employing *inductance*, *resistance*, or *capacity*. They are the building blocks of electrical engineering.

The use of inductances permitted the development of transformers, electromagnets, electric motors, generators and similar appliances.

The use of resistors made possible the development of electric lights, electric heaters, controls, and the like.

But modern electrical engineering would have been impossible without the use of condensers—millions of condensers, of many types and sizes—some of them not much larger than a match head, others as big as a room.

THE COMING OF THE MODERN CONDENSER

The condenser is an old invention but a recent development.

The first electrical condenser, the Leyden jar, was invented in 1746 by Deen Van Kleist. It was referred to by Benjamin Franklin as an "accumulator" of electrical energy. Later, it was used extensively in medical and wireless telegraph equipment. The Leyden jar remained practically unchanged for more than 200 years, retaining essentially the same shape, design and construction.

Forty years ago, in 1910, we already had a sizable electrical industry—all of it based on electrical devices employing primarily only inductance and resistance. The only practical power condenser then available was the glass Leyden jar, or its equivalent, the glass plates.

* Based on a paper presented before the Seminar of Electrical Engineering, Princeton University, Princeton, N. J., February 28, 1949.

[1] Founder and Technical Director, Cornell-Dubilier Electric Co., New York, N. Y.

(Note—The Franklin Institute is not responsible for the statements and opinions advanced by contributors in the JOURNAL.)

The telephone and telegraph industry, operating with only minute energies, had a primitive low-voltage, low-power paper condenser. For higher voltages and higher powers we used glass plates, or the equally inefficient, cumbersome, fragile Leyden jars.

The standard, fragile glass jar was then used in the many thousands of high-tension electro-medical machines, in thousands of wireless telegraph installations. Radio communications with ships at sea, and between the ships of all the navies of the world, all depended on the Leyden jars.

Here is an interesting footnote to history. Up to the end of 1911, practically all of the Leyden jars were made in Germany. All commercial and military radio installations used German-made Leyden jars. The German government subsidized the industry and discouraged foreign development.

The British Navy realized that its entire communications system was dependent on a foreign power. When I was visiting England in 1911, the government invited me to assist them in finding a substitute for the Leyden jar. Thus the modern power capacitor was born.

THE ROCKY ROAD OF PROGRESS

We began with crude tools. We were lone workers, shaping the individual bricks of knowledge. Today, the edifice of knowledge is a towering vastness: new bricks are being added daily, raising it ever higher—and I doubt that a single human mind could encompass all the knowledge it contains. We did not know nearly as much about electrons and atomic structure as we do today; wave mechanics were nearly two decades in the future.

In the beginning, our progress was slow. We gained new knowledge experimentally, by trial and error. This gave us experience and developed our imagination. Experience and imagination make an ideal marriage.

The rocky road of progress is hard. There are many obstacles to be overcome, and the inertia of public opinion is not the least of these. If radio broadcasting had been developed before the telephone, and then someone had invented a method of making broadcasting secret, by simply guiding the waves along a thin metal wire, he would have received public acclaim.

A little more than a century ago, when trains were first developed, a speed of twelve miles an hour was considered the limit of human endurance. The medical profession, newspapers and others, were quick to point out their terrible menace and danger to humanity. They predicted that a speed of fifteen miles an hour would cause nosebleeds, deafness and even death.

I recall that in my own boyhood, automobiles were prohibited in many sections: they frightened horses, and a speed of twenty-five

miles an hour—"without tracks," as an old ordinance put it—was "dangerous." There were local laws to keep automobiles off the roads; and there was broken glass to cut our tires, and stretched wire to cut our necks. The man who first drove an automobile through Central Park in New York was arrested for disorderly conduct.

Long ago, when I was a lad, a bearded German professor named Roentgen discovered some mysterious X-rays which made it possible to photograph bones in the living body. The now-defunct *Pall Mall Gazette*, of London, was horrified. It protested against what it called

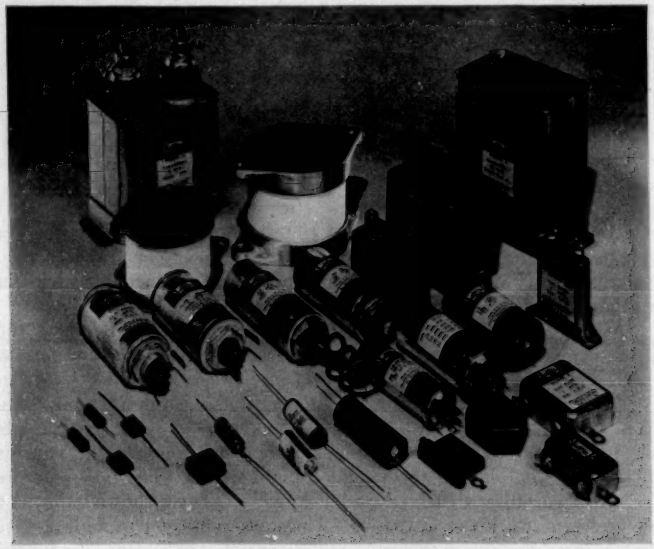

FIG. 1. Representative group of small electrical condensers showing variety of shapes and sizes.

the "revolting indecency of making pictures of our insides," and hoped something would be done to "thwart the shameless experimenters who were beginning to supply the discovery." This newspaper stated that it would be possible to see through the clothes of people as they walked in the streets.

We, too, had similar obstacles to overcome.

The condenser appears to be the simplest of all electrical devices—a pair of conducting sheets separated by insulating layers. Actually, the condenser is probably the most complex of the electrical elements.

It has more hidden problems than any other electrical device, and is more difficult to produce.

Today, we take our condensers for granted, and expect them to do their job with precision. We can do so only because much ingenuity and many inventions resulting from patient research went into their design and construction.

The eventual adoption of the new compact and efficient power capacitors permitted the development of many branches of the electrical industry, with its high-frequency equipment and vacuum tube applications. Powerful broadcasting and communications stations, and other high-frequency equipment, would have been impractical because of the prohibitive size, cost and inefficiency of the glass jar.

THE MICA CAPACITOR

The first development that broke the German Leyden-jar monopoly was our *mica condenser*.

Up to 1910, all technical publications and text-books were in agreement that mica was, theoretically, a more efficient and suitable material than glass. Yet there was no practical mica condenser, one that could withstand for long periods of time high voltages or high power without deterioration and breakdown. The phenomena of corona, hysteresis, eddy currents, ionization, and above all mechanical losses in capacitors, were either misinterpreted or unknown.

In those days whenever higher voltages were involved, it was the customary practice to make the insulating material thicker and larger.

I found that corona, or brush discharge, was particularly destructive, and that it invariably started at potentials of around 1000 volts. To overcome this, I did not "make it thicker and larger." We made and tested hundreds of condensers, employing materials of various thicknesses, applying to them different potentials. These condensers were then carefully dissected and examined. Tests showed that, at five times the thickness of the insulating material, the corona began at *less than two times* the previous corona potential. I therefore concluded that the voltage across any two adjacent electrodes must always be less than 1000, irrespective of the total voltage applied to a condenser. This was the origin of the corona-free condenser.

After the corona was eliminated, some condensers still became hot and broke down. We found that in some cases certain spots in the armatures became discolored because of concentrated heat.

I recalled my school days and the teacher's demonstration of the "talking book" telephone. The "talking book" was a loosely arranged condenser made by placing light metal foils between the pages of a book. When connected to a microphone and a battery, the book "talked." I connected the book across a 60-cycle supply, and it gave

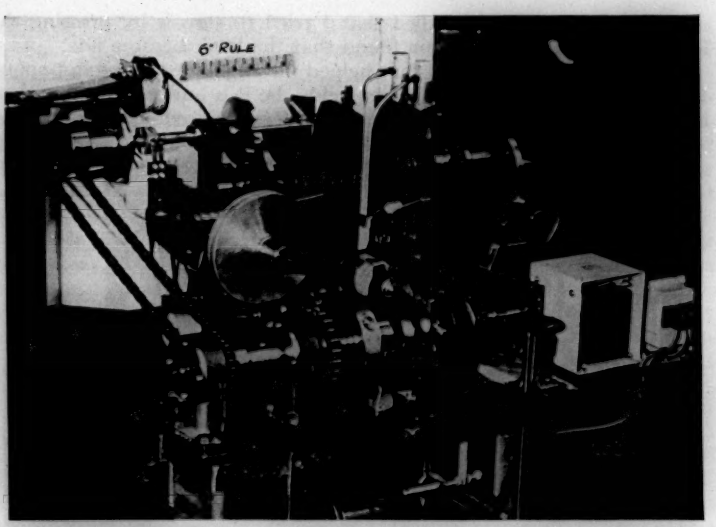

FIG. 2. An automatic machine for making mica condensers.

FIG. 3. Finished condensers being ejected from the machine shown in Fig. 2.

a tremendous hum. I recalled that I tried to stop it by pressing the book with my hand, and soon found that the book became hot.

It was this school lesson that helped me to eliminate the hot spots. I reasoned that, whatever the frequency, be it a hundred thousand or half a million cycles instead of sixty or a few hundred, a minute move-

FIG. 4. The author, with a large mica condenser rated at 2250 KVA. for operation at 15,000 volts, 150 amperes.

ment of the electrodes resulted in heavy power losses. Hence, it was necessary to obtain an intimate contact between the foil electrodes and the mica sheets.

I found that the surface of mica sheets, although it appears perfectly smooth to the eye, is in reality full of microscopic hills and dales. Therefore, a special type of soft metal foil was developed, one that would flow and imbed itself into the fine crevices of the mica sheets, ensuring an intimate contact throughout the condenser. This was the second major improvement which made the mica condenser practical.

With heavy currents, such as are encountered in high-frequency equipment, X^2R loss became a serious factor. To reduce this loss to a minimum, changes were made in the shapes, sizes, and assembly. The units were evacuated and impregnated with certain compounds at various temperatures. We were able to reduce the size of the mica condenser to less than 10 per cent of the equivalent Leyden jar, and the losses by more than 90 per cent.

Ours being a new development, we were subjected to most rigid specifications. Although the size (and therefore the radiating surface) was considerably reduced, and consequently heat generation due to losses was also reduced, instead of allowing us a temperature rise equivalent to that allowed in Leyden jars, we were limited to 10° C., in places where the equivalent Leyden jar became so hot that many times the glass melted, and cooling fans were therefore necessary.

Not only did we reduce the overall dimensions of the capacitor, but we also eliminated a great deal of such associate equipment. The importance of this can be realized when we recall that in a radio installation on board a battleship, Leyden jars usually occupied more than 50 per cent of the equipment space.

For a while, the government distrusted our new and revolutionary condenser, as lives and ships depended on its continued safe operation. To meet the exacting government specifications, we produced units where the heat radiation was equal to the heat generation, and thermal stability was reached within less than 10° C.

Today, it is a source of some satisfaction to us that every radio broadcasting station, every radio transmitting station on land, at sea or in the air, and other high-frequency electrical equipment use mica condensers as originated by us forty years ago.

PAPER CONDENSERS

Paper condensers employ impregnated paper as the dielectric. Paper condensers look quite simple, but their appearance is deceiving. They are extremely difficult to engineer and produce.

Consider the paper that serves as the dielectric. Many of our capacitors contain enough paper to cover the walls of a room. A

single microscopic defect, a mere pinpoint, will cause the entire condenser to fail. In a modern condenser factory, the materials controls which apply to the paper begin with the manufacturer of the paper itself. He must carefully control the chemical content of the water used for washing the pulp from which the paper will be made. He must control, within close limits, the ash content, the acidity, the alkalinity, the porosity, and the residual moisture in the finished product. Minute metal particles from paper-making machines find their way into the paper, impairing its dielectric efficiency. Paper thickness is exceedingly important, as the cost and the bulk of condensers increase as the square of the thickness.

FIG. 5. Winding paper condensers.

The design of metal electrodes, and the composition of the metal foil, are equally important. Under certain operating conditions, metal particles detach themselves from the foil and penetrate the paper, resulting in disintegration and breakdown of the condenser. Aluminum foil has been found to minimize such ionic effects.

Paper condensers are impregnated with various insulating materials, such as waxes, oils, chlorinated diphenyl preparations, and others. These must be constantly tested before using, and must be free from contamination. Blending some of the impregnants results in improve-

ments; other blends produce poor results. Condensers are impregnated under vacuum, and the production cycle sometimes takes more than 150 hr. The vacuum is as low as 100 microns, and the temperatures are about 250° F.

The manufacture of paper condensers is a controlled precision operation from start to finish. Materials must be kept free from contamination. We must even guard ourselves against the effect of perspiration of the assembly workers.

The fibrous paper and the impregnants alike have a great affinity for moisture. Unless thoroughly sealed, they can absorb a great deal of moisture from the atmosphere. On an ordinary humid day, in a few hours the units may become unfit for use. To guard against moisture absorption, paper condensers are assembled and impregnated under carefully controlled conditions, and then hermetically sealed. The seal itself must withstand the internal expansion and contraction over a wide temperature range.

There are many other, unseen dangers. A slightly defective condenser may operate satisfactorily for a length of time, but under power strains, internal heat is generated due to the various losses. Unless proper precautions are taken, fatty acids may be formed inside the unit. In many instances, inhibitors must be added to the impregnants.

The completed unit is tested at approximately twice its normal operating voltage, and its terminals at five times. It is then passed through long heated ovens for detection of minute flaws. Finally, the unit is given an accelerated heat test under power overload.

These are only some of the problems in paper condenser manufacture. Many other, unforeseen problems arise, which must be solved.

Here is an interesting puzzle that gave us many a sleepless night. We made a large number of paper condensers, rated at 600 volts, for a new high-voltage anode supply source operating over long continuous periods. Before shipment, our condensers were all tested at 6000 volts. The breakdown tests showed more than 10,000 volts. The condensers were impregnated with a refined paraffin wax, as we had practiced successfully for many years, and under normal conditions would have lasted almost indefinitely.

A few months later, many of these condensers failed in service and were returned to us. We were mystified. Investigation showed that dark streaks and spots had developed on the paper inside the condensers. It took much time and work to analyze and solve this riddle.

We discovered that when the condenser units were removed from the impregnating tanks, the outside of the units cooled rapidly and formed a hard solid shell. But the center retained its heat for a much longer period, keeping the wax soft and fluid. As the center finally cooled and contracted, minute spaces were formed *internally*, sealed by the solid outer crust. Gases filled these spaces, and the gases glowed

at potentials of 200 volts or less. Our condensers, in effect, contained miniature glow lamps.

When subjected to long continued periods of operation, enough heat was generated to destroy the insulation, causing breakdowns. In addition, the uneven contraction of the wax also imposed severe mechanical strains and distortion along the insulating layers. Thus, condensers made to operate reliably at thousands of volts may break down at a potential of a few hundred volts, unless precautions are taken to prevent ionic discharges within the unit.

This was a serious problem, and one that we had to overcome at once. Finally, one of my assistants suggested cooling the condensers under oil. This allowed the entire impregnated mass to cool without the hard shell.

This cooling process increased the life of the condenser tenfold, and its rated safe operating voltage from three to five times. This simple manufacturing improvement proved to be one of the most important and revolutionary developments in wax-impregnated condensers, and now is universally used in the manufacture of high-voltage capacitors.

ELECTROLYTIC CONDENSERS

Up to 1925, one of the basic precautions taught to every condenser worker was to be always on guard against any risk of contamination of condenser materials by outside chemicals—alkalis or acids. We knew, from our own sad experiences, that a single drop of water or acid in a gallon of impregnating oil or wax would make the entire batch of material unfit for use.

We were so thoroughly trained in strict precautions against chemical contamination of our condenser materials, that the very idea of making a *chemical* condenser seemed at first frightening. Although we knew that metallic oxides were good insulators, we also knew that strong acids are needed for the formation of such oxides on aluminum foil—and strong acids could never be tolerated in or near a condenser plant.

These were the mental roadblocks that the new electrolytic condenser had to overcome. Yes, we were slow and cautious in accepting the electrolytic condenser. But today, it has found its rightful place in industry, especially for starting small a-c. motors, and in filtering circuits.

Although the electrolytic condenser seems to the eye to be much more complex, the problems of its manufacture are nowhere near as great as those of mica and paper condensers.

CERAMIC CONDENSERS

During the First World War, the Germans purchased, through Holland, a small number of our transmitting condensers, and copied them, Japanese fashion. Those were shipped by us in 1916, and I knew that they were destined for Germany. After the War, in 1920,

I visited Berlin. The Telefunken Company, which was then the largest radio organization in the world, showed me thousands of units made exactly like ours. Most of them failed after a few weeks' service. I knew they would fail—another proof that experience is necessary for success.

Ceramic condensers originated in England, about a quarter of a century ago. However, they received their highest development in Germany, after the First World War—again with the aid of financial subsidies from the German government.

At the end of the First World War, the new mica condensers were used extensively, in transmitters and other electrical equipment. Germany had no mica supply of her own. The best mica came mostly from England and India. Therefore, Germany heavily subsidized and encouraged the development of ceramics to replace mica.

The resultant ceramics were much stronger and had lower losses than the old wet-process porcelains. Units were made of many materials, such as magnesium, and later the titanates. Their production required higher firing temperatures and closer manufacturing tolerances and controls.

The development of low-loss ceramic insulators, particularly those with high-capacitance possibilities, soon affected the electric power industry.

Ceramic condensers were gradually improved until the overall efficiency of the best German-made condensers during the last War was about equal to mica condensers of similar dimensions.

Since then, American manufacturers concentrated on the development of titanates, mostly for use in low-voltage applications. Titanate compounds have the advantage of possessing a large capacity, and occupy but a small space.

We have made some ceramic condensers with a K as high as 500,000. The losses, however, were more than 30 per cent. (The K of mica is about 7; that of paper, around 4; of paraffin, around 2.)

Improvement in ceramic condensers has been rapid. At present, large quantities of ceramic condensers are being made, with a K of between 3000 and 5000, with losses as low as 2 per cent. Recent developments in low-loss ceramics show most encouraging results.

WHAT OF THE FUTURE?

The future progress in electricity and radio is inseparable from progress in condenser design.

Inductances and resistances have never presented serious design or manufacturing problems: they are not likely to present them in the future. But the third of the building blocks of electrical engineering—the condenser—remains a limiting factor in applied electrical and radio engineering.

Forty years ago, our horizons limited by the old Leyden jar, we could not foresee the variety, the complexity, the utility of modern electrical apparatus. New and better condensers were a major factor in making the modern electrical and radio industry possible. Today, forty years later, our eyes can see farther, and our vision is clearer. With our mind's eye we can see the magnificent vistas which the development of newer and better condensers may bring about comparatively few years from now.

There always is something newer and better waiting to be developed. Forty years ago, the new compact mica capacitor replaced the Leyden jar. Today, its supremacy is already threatened by the newer types, such as for instance the ceramic capacitor, and the yet-newer vacuum-tube type. And yet, such is the excellence of the modern mica condenser that it will never be eliminated or supplanted by others; rather, the newer capacitors will open new fields, will make possible new apparatus as yet in the dream stage.

It is a thankless task to prophesy; but, given capacitors smaller and more efficient than the best we have today, such obvious new devices as vest pocket telephone transmitters, capable of reaching a relay station a few miles away, would be a practical possibility. Those same condensers would also permit us not merely to bounce a few radar pulses against the surface of the moon, as was done some two years ago, but to maintain communications with the space ships which will inevitably venture forth in a few years, ranging farther afield than the moon, into the solar system, perhaps beyond.

V.24
1949

ENERGY FLUCTUATIONS IN A VAN DER POL OSCILLATOR

BY

N. MINORSKY, Ph.D.[1]

1. INTRODUCTION

By analogy with the differential equation of the harmonic oscillator

$$\ddot{x} + x = 0 \tag{1.1}$$

one can consider the equation

$$\ddot{x} - \epsilon(1 - x^2)\dot{x} + x = 0 \tag{1.2}$$

as representing a special, *van der Pol oscillator* (abbreviation VDP). The important feature of the harmonic oscillator is the fact that (1.1) has the first integral

$$\tfrac{1}{2}\dot{x}^2 + \tfrac{1}{2}x^2 = h, \tag{1.3}$$

which expresses the law of conservation of energy (we assume here for the sake of simplicity $m = c = \omega_0 = 1$ in the usual form of the equation $m\ddot{x} + cx = 0$ of the harmonic oscillator).

Although the VDP oscillator does not possess this feature, the introduction of *energy* as a dependent variable is of a certain interest in applications and this will form the subject of this note.

If one uses the phase-plane representation ($\dot{x} = y$), (1.3) is

$$x^2 + y^2 = r^2 = \rho = 2h. \tag{1.4}$$

That is, $r^2 = \rho$ represents twice the total energy of the harmonic oscillator and, moreover, this energy is constant throughout the cycle. In order to simplify the writing we will assume that $r^2 = \rho = 2h$ is the total energy of the oscillator thus disregarding the factor 2.

Equation 1.1 written as a system of two equations is

$$\dot{x} = y; \qquad \dot{y} = -x.$$

Transforming these equations into ρ, θ coordinates one gets:

$$\frac{d\rho}{dt} = 0; \qquad \frac{d\theta}{dt} = -1. \tag{1.5}$$

Eliminating time between these equations one obtains the integral curve (or "trajectory")

$$\frac{d\rho}{d\theta} = 0. \tag{1.6}$$

[1] Department of Electrical Engineering, Stanford University, Stanford, Calif.

The first equation (1.5) expresses the law of conservation of energy; (1.6) represents a circle in the ρ, θ plane and the second equation (1.5) gives $\theta = -t$, as the constant of integration can obviously be assumed to be zero by a proper choice of the origin of either θ or t. The sign minus appearing in this equation is of no special significance and arises merely from the fact that the angles are counted as positive in the trigonometric sense (counterclockwise) while positive direction on the integral curve is clockwise.

If one applies this procedure to (1.2) one obtains similar equations

$$\frac{d\rho}{dt} = 2\epsilon(1 - \rho \operatorname{Cos}^2 \theta)\rho \operatorname{Sin}^2 \theta, \tag{1.7}$$

$$\frac{d\theta}{dt} = -1 + \epsilon(1 - \rho \operatorname{Cos}^2 \theta) \operatorname{Sin} \theta \operatorname{Cos} \theta, \tag{1.8}$$

$$\frac{d\rho}{d\theta} = \frac{2\epsilon(1 - \rho \operatorname{Cos}^2 \theta)\, \rho \operatorname{Sin}^2 \theta}{\epsilon(1 - \rho \operatorname{Cos}^2 \theta) \operatorname{Sin} \theta \operatorname{Cos} \theta - 1}. \tag{1.9}$$

These equations reduce to Eqs. 1.5 and 1.6, respectively, when $\epsilon = 0$. Since it is known that the VDP oscillator is periodic, its integral curve is closed, that is

$$\int_0^{2\pi} \frac{d\rho}{d\theta} d\theta = \int_0^{2\pi} d\rho = 0. \tag{1.10}$$

If, moreover, $\epsilon \ll 1$ the VDP oscillator differs but little from a harmonic oscillator so that $\rho(\theta) \cong \rho_0 = \text{Const.}$ In this case neglecting the small term with ϵ in the denominator of (1.9) one can write

$$\frac{d\rho}{d\theta} \cong -2\epsilon(1 - \rho_0 \operatorname{Cos}^2 \theta)\rho_0 \operatorname{Sin}^2 \theta,$$

and the condition (1.10) of periodicity gives

$$\int_0^{2\pi} d\rho = -2\epsilon\left[\rho_0 \int_0^{2\pi} \operatorname{Sin}^2 \theta d\theta - \rho_0^2 \int_0^{2\pi} \operatorname{Cos}^2 \theta \operatorname{Sin}^2 \theta d\theta \right] = 0, \tag{1.11}$$

whence $\rho_0 = r_0^2 = 4$, which is well known (1).[3] If, however, $\epsilon = 0$, condition (1.10) is satisfied identically in (1.11) and one has no right to equate the square bracket in (1.11) to zero. In this case ρ_0 cannot be determined from (1.11) which is also obvious since in this case the VDP oscillator degenerates into a harmonic oscillator whose energy content is arbitrary depending on the initial conditions: For a VDP oscillator, on the contrary, the initial conditions ultimately do not play any role and the oscillator "selects," so to speak, a definite energy content $\rho_0 = 4$ as long as $\epsilon \ll 1$ but not zero.

So far we were able merely to retrace some well-known facts,

[3] The boldface numbers in parentheses refer to the references appended to this paper.

starting with a new dependent variable ρ, the energy. In what follows we shall endeavor to elaborate this line of argument.

2. PHASE TRAJECTORY

We will consider first the differential equation (1.9) of the phase trajectory assuming $\epsilon \ll 1$. Expanding the right hand of (1.9) into a series one gets

$$\frac{d\rho}{d\theta} = -2\rho[\epsilon(1 - p\,\mathrm{Cos}^2\,\theta)\,\mathrm{Sin}^2\,\theta + \epsilon^2(1 - \rho\,\mathrm{Cos}^2\,\theta)^2 \times \\ \times \mathrm{Sin}^3\,\theta\,\mathrm{Cos}\,\theta + \epsilon^3(1 - \rho\,\mathrm{Cos}^2\,\theta)^3\,\mathrm{Sin}^4\,\theta\,\mathrm{Cos}^2\,\theta + \cdots], \quad (2.1)$$

where $\rho = \rho(\theta)$ is an unknown periodic function of θ which we will endeavor to determine by the perturbation method. If one sets $\rho = \rho_0 + \epsilon\rho_1 + \epsilon^2\rho_2 + \cdots$ in the preceding equation, one obtains a series of successive approximations arranged according to the order of ϵ.

(*a*) *Approximation of order zero*

$$\frac{d\rho_0}{d\theta} = 0; \qquad \rho_0 = K_0 = \mathrm{Const.}$$

(*b*) *First approximation*

From (2.1) one has

$$\frac{d\rho_1}{d\theta} = -2(1 - \rho_0\,\mathrm{Cos}^2\,\theta)\rho_0\,\mathrm{Sin}^2\,\theta,$$

whence

$$\rho_1 = K_1 - \rho_0(1 - \tfrac{1}{4}\rho_0)\theta + \tfrac{1}{2}\rho_0\,\mathrm{Sin}\,2\theta - \tfrac{1}{16}\rho_0^2\,\mathrm{Sin}\,4\theta, \quad (2.2)$$

K_1 being an integration constant. The second term on the right of (2.2) is clearly a *secular term* and cannot exist in a stationary state. Determining the constant ρ_0 so as to eliminate this term one obtains again $\rho_0 = 4$ so that (2.2) becomes

$$\rho_1 = K_1 + 2\,\mathrm{Sin}\,2\theta - \mathrm{Sin}\,4\theta. \quad (2.3)$$

The constant K_1 is determined in the next approximation.

(*c*) *Second approximation*

Equating the terms with ϵ^2 in (2.1) one obtains

$$\frac{d\rho_2}{d\theta} = -2\rho_1\,\mathrm{Sin}^2\,\theta + 4\rho_1\rho_0\,\mathrm{Sin}^2\,\theta\,\mathrm{Cos}^2\,\theta - 2\rho_0\,\mathrm{Sin}^3\,\theta\,\mathrm{Cos}\,\theta + \\ + 4\rho_0^2\,\mathrm{Sin}^3\,\theta\,\mathrm{Cos}^3\,\theta - 2\rho_0^2\,\mathrm{Sin}^3\,\theta\,\mathrm{Cos}^5\,\theta.$$

Replacing ρ_1 and ρ_0 by their values, passing to the multiple arguments, integrating, and eliminating the secular term (which yields $K_1 = 0$)

one gets

$$\rho_2 = K_2 - \frac{3}{4}\operatorname{Cos} 2\theta + \frac{1}{4}\operatorname{Cos} 4\theta + \frac{5}{12}\operatorname{Cos} 6\theta - \frac{1}{4}\operatorname{Cos} 8\theta, \quad (2.4)$$

where K_2 is a constant of integration.

(*d*) *Third approximation*

One obtains $K_2 = \frac{3}{8}$ and

$$\rho_3 = -\frac{1}{12}\operatorname{Sin} 2\theta - \frac{5}{192}\operatorname{Sin} 4\theta + \frac{23}{72}\operatorname{Sin} 6\theta - \frac{37}{192}\operatorname{Sin} 8\theta - \frac{5}{48}\operatorname{Sin} 10\theta + \frac{5}{64}\operatorname{Sin} 12\theta + K_3. \quad (2.5)$$

If one limits the approximation up to the terms of the order ϵ^4, the periodic function $\rho(\theta)$ is then given by the following expression arranged by the orders of ϵ:

$$\begin{aligned}\rho(\theta) = 4 &+ \\ &+ \epsilon(2\operatorname{Sin} 2\theta - \operatorname{Sin} 4\theta) + \\ &+ \epsilon^2\left(\frac{3}{8} - \frac{3}{4}\operatorname{Cos} 2\theta + \frac{1}{4}\operatorname{Cos} 4\theta + \frac{5}{12}\operatorname{Cos} 6\theta - \frac{1}{4}\operatorname{Cos} 8\theta\right) + \\ &+ \epsilon^3\left(K_3 - \frac{1}{12}\operatorname{Sin} 2\theta - \frac{5}{192}\operatorname{Sin} 4\theta + \frac{23}{72}\operatorname{Sin} 6\theta - \frac{37}{192} \times \right. \\ &\qquad \left. \times \operatorname{Sin} 8\theta - \frac{5}{48}\operatorname{Sin} 10\theta + \frac{5}{64}\operatorname{Sin} 12\theta\right) + \\ &+ \cdots.\end{aligned} \quad (2.6)$$

If the terms of this array are arranged according to the order of harmonics one gets

$$\begin{aligned}\rho(\theta) = (4 + \tfrac{3}{8}\epsilon^2 + \cdots) + \\ &+ \left[\left(2\epsilon - \frac{1}{12}\epsilon^3 + \cdots\right)\operatorname{Sin} 2\theta + \left(-\frac{3}{4}\epsilon^2 + \cdots\right)\operatorname{Cos} 2\theta\right] + \\ &+ \left[\left(-\epsilon - \frac{5}{192}\epsilon^3 + \cdots\right)\operatorname{Sin} 4\theta + \left(\frac{1}{4}\epsilon^2 + \cdots\right)\operatorname{Cos} 4\theta\right] + \\ &+ \left[\left(\frac{23}{72}\epsilon^3 + \cdots\right)\operatorname{Sin} 6\theta + \left(\frac{5}{12}\epsilon^2 + \cdots\right)\operatorname{Cos} 6\theta\right] + \\ &+ \left[\left(-\frac{37}{192}\epsilon^3 + \cdots\right)\operatorname{Sin} 8\theta + \left(-\frac{1}{4}\epsilon^2 + \cdots\right)\operatorname{Cos} 8\theta\right] + \\ &+ \cdots.\end{aligned} \quad (2.7)$$

The non-written terms in brackets are ascending powers of ϵ. Unfortunately, the calculations beyond the third approximation are so

V.24
1949

long that it becomes impracticable to continue them unless, perhaps, with the aid of some mechanical computers. It is possible, however, to form certain general conclusions regarding the series (2.7).

1. The coefficients $a_0, a_1, b_1, a_2, b_2 \cdots$ of the trigonometric terms in (2.7) are power series in ϵ approaching zero when $\epsilon \to 0$, except a_0 which approaches the value 4. The amplitudes $\sqrt{a_1^2 + b_1^2} \cdots$ of the various harmonics also approach zero when $\epsilon \to 0$. As to their phases, they approach at the limit $\epsilon \to 0$ the phase of the term whose coefficient contains a lower power of ϵ.

2. It seems likely (although the approximations in our case did not progress far enough to be able to assert this) that for a sufficiently small ϵ, the coefficients a_n, b_n of the trigonometric series (2.7) approach zero when $n \to \infty$. If such is the case the trigonometric series (2.7) is actually a Fourier series.

3. The constant term $(4 + \frac{3}{8}\epsilon^2 + \cdots)$ may be regarded as a "component" of a harmonic oscillator while the trigonometric terms represent merely the *energy fluctuations* between the VDP oscillator and the external source. It should be noted that the preceding discussion relates only to the integral curve $\rho(\theta)$ of the VDP oscillator inasmuch as *time* does not enter here. In the following section we shall investigate the dependence on time, that is, the actual fluctuations of energy. It may be useful to say a few words regarding the convergence of the expansion (2.1). Inasmuch as this expansion was obtained from the function appearing on the right side of (1.9) it is clear that the only case when it is divergent is when $d\theta/dt = 0$. This case is obviously ruled out for $\epsilon \ll 1$ in which we are interested here. It can be shown, however, (section 5 below) that, even in the case when ϵ is large, $d\theta/dt \neq 0$ although it may become of the order of $1/\epsilon^2$ for some special intervals of θ. In these intervals the convergence becomes so slow that the perturbation method becomes impracticable in view of the impossibility of carrying the subsequent approximations indefinitely on account of a rapidly increasing complexity of calculations.

For this reason the preceding procedure is applicable only for $\epsilon < 1$ and, preferably, for $\epsilon \ll 1$. In many applications, however, one is interested precisely in the range of small ϵ so that the perturbation procedure can be used then. As regards the so-called "relaxation range" ($\epsilon \gg 1$), although the perturbation method ceases to be applicable, the energy fluctuations in a VDP oscillator can be still explored in connection with the data obtained by the isocline method as will be shown in section 5.

3. ENERGY FLUCTUATIONS

The preceding study concerns the function $\rho(\theta)$ in which the time does not appear. In order to investigate the energy fluctuations $\rho(t)$ in

a VDP oscillator it is necessary to deal directly with Eqs. 1.7 and 1.8 containing time. In other words, it is necessary to determine the *motion* $\rho(t)$ on the trajectory $\rho(\theta)$.

The perturbation procedure remains the same as before with the exception that it is to be carried out simultaneously in both variables ρ and θ considered as functions of time.

Equations 1.7 and 1.8 can be written

$$\frac{d\rho}{dt} = \epsilon[\rho(1 - \operatorname{Cos} 2\theta) - \tfrac{1}{4}\rho^3(1 - \operatorname{Cos} 4\theta)], \tag{3.1}$$

$$\frac{d\theta}{dt} = \epsilon[(\tfrac{1}{2} - \tfrac{1}{4}\rho) \operatorname{Sin} 2\theta - \tfrac{1}{8}\rho \operatorname{Sin} 4\theta] - 1. \tag{3.2}$$

Since the time does not appear explicitly in these equations, there is no difference between t and $t + t_0$, t_0 being arbitrary. This means that to a given trajectory (or integral curve) $\rho(\theta)$ corresponds an infinity of motions $\rho(t)$, $\theta(t)$ differing by an arbitrary phase t_0 depending on the initial conditions.

The perturbation procedure is carried out by setting

$$\rho = \rho_0 + \epsilon\rho_1 + \epsilon^2\rho_2 + \cdots,$$
$$\theta = \theta_0 + \epsilon\theta_1 + \epsilon^2\theta_2 + \cdots.$$

Since θ appears only under the sign of the trigonometric functions we have to expand Sin 2θ, Cos 2θ, $\cdots$ into a Taylor's series around $\theta = \theta_0$, which gives

$$\operatorname{Cos} 2\theta = \operatorname{Cos} 2\theta_0 - 2(\epsilon\theta_1(t) + \epsilon^2\theta_2(t) + \cdots) \operatorname{Sin}\ 2\theta_0 + \cdots,$$
$$\operatorname{Sin}\ 2\theta = \operatorname{Sin}\ 2\theta_0 + 2(\epsilon\theta_1(t) + \epsilon^2\theta_2(t) + \cdots) \operatorname{Cos} 2\theta_0 + \cdots.$$

Rearranging the results according to the powers of ϵ one finds

$$\begin{aligned}\frac{d\rho}{dt} = {} & \epsilon[\rho_0(1 - \operatorname{Cos} 2\theta_0) - \tfrac{1}{4}\rho_0^3(1 - \operatorname{Cos} 4\theta_0)] + \\ & + \epsilon^2[2\rho_0\theta_1 \operatorname{Sin} 2\theta_0 + \rho_1(1 - \operatorname{Cos} 2\theta_0) - \\ & - \rho_0^2\theta_1 \operatorname{Sin} 4\theta_0 - \tfrac{1}{2}\rho_0\rho_1[1 - \operatorname{Cos} 4\theta_0)] + \epsilon^3[\cdots] + \cdots\end{aligned} \tag{3.3}$$

$$\begin{aligned}\frac{d\theta}{dt} = {} & -1 + \epsilon[(\tfrac{1}{2} - \tfrac{1}{4}\rho_0) \operatorname{Sin} 2\theta_0 - \tfrac{1}{8}\rho_0 \operatorname{Sin} 4\theta_0] + \\ & + \epsilon^2[(1 - \tfrac{1}{2}\rho_0)\theta_1 \operatorname{Cos} 2\theta_0 - \tfrac{1}{4}\rho_1 \operatorname{Sin} 2\theta_0 - \\ & - \tfrac{1}{2}\rho_0\theta_1 \operatorname{Cos} 4\theta_0 - \tfrac{1}{8}\rho_1 \operatorname{Sin} 4\theta_0] + \epsilon^3[\cdots] + \cdots.\end{aligned} \tag{3.4}$$

The approximation of the zero order yields again

$$\frac{d\rho_0}{dt} = 0; \qquad \frac{d\theta_0}{dt} = -1, \qquad \text{that is} \qquad \theta_0 = -t,$$

which coincides with Eqs. 1.5 for the harmonic oscillators. The elimination of the secular term in the first approximation gives again $\rho_0 = 4$. There appears, however, another constant of integration in the second equation which must be determined by the *initial conditions*, the independent variable being now t. The simplest way of introducing the initial condition is to assume that for $t = 0$, $\theta(0) = \theta_1(0) = \theta_2(0) = \cdots = 0$.

The first approximation becomes then

$$\rho_1(t) = K_1 - 2 \operatorname{Sin} 2t + \operatorname{Sin} 4t;$$
$$\theta_1(t) = \tfrac{3}{8} - \tfrac{1}{4} \operatorname{Cos} 2t - \tfrac{1}{8} \operatorname{Cos} 4t, \qquad (3.5)$$

where K_1 is an integration constant determined in the second approximation. The procedure from now on becomes obvious, *viz:* for the second approximation we collect the terms with ϵ^2 in (3.3) and (3.4) and it is observed that $d\rho_2/dt$ and $d\theta_2/dt$ are expressible now in terms of ρ_0, θ_0, ρ_1 and θ_1. Integrating these equations, eliminating the secular term in ρ_2 (which leads to the determination of K_1) and determining the constant of integration in θ_2 by the assumed initial conditions, one obtains the second approximation ρ_2 and θ_2; one finds

$$\rho_2 = K_2 + \operatorname{Cos} 2t - \frac{7}{4} \operatorname{Cos} 4t + \frac{2}{3} \operatorname{Cos} 6t,$$

where $K_1 = 0$.

It is to be noted that the expression for $\rho_2(t)$ is not the same as that for $\rho_2(\theta)$ and likewise for other approximations so that, in general, the trigonometric series for $\rho(t)$ is not the same as that for $\rho(\theta)$. The reason for that is due to the non-uniformity of rotation of the radius vector as is seen from the expression for $\theta_1(t)$ which gives in this approximation

$$\theta = -t + \epsilon(\tfrac{3}{8} - \tfrac{1}{4} \operatorname{Cos} 2t - \tfrac{1}{8} \operatorname{Cos} 4t).$$

This shows that there exists a kind of a "phase modulation" affecting all trigonometric terms.

The fluctuation of energy in time up to the terms of the order ϵ^3 is then

$$\rho(t) = 4 + \epsilon(-2 \operatorname{Sin} 2t + \operatorname{Sin} 4t) + \\ + \epsilon^2 \left(\operatorname{Cos} 2t - \frac{7}{4} \operatorname{Cos} 4t + \frac{2}{3} \operatorname{Cos} 6t \right) + K_2,$$

where the constant of integration K_2 is determined in the next approximation and so on.

4. EFFECT OF THE FORM OF THE VAN DER POL EQUATION ON THE FREQUENCY SPECTRUM

So far we have been concerned with Eq. 1.2 originally formulated by van der Pol (1). Later on, this equation was generalized by A.

Liénard (2), E. & H. Cartan (3), N. Levinson and O. K. Smith (4) and others. The general form of the van der Pol equation is

$$\ddot{x} - \epsilon f(x, \dot{x})\dot{x} + g(x) = 0, \tag{4.1}$$

where the functions f and g must satisfy certain conditions (4). We shall give a few examples relative to the electron tube circuits assuming that they do not involve any non-linear capacities in which case $g(x) = x$, and consider $f(x, \dot{x}) = f(x)$ in the Liénard sense, *viz:* $f(x)$ is an even function of x so that $F(x) = \int f(x)dx$ is odd and positive for small values of x and becomes negative beginning with $x = x_0$, decreasing monotonically for $x > x_0$. The polynomials of the form $F(x) = ax - bx^3$; $F(x) = ax + bx^3 - cx^5$ etc., clearly, satisfy this condition and are frequently used in applications. Thus, for instance, when $F(x)$ is a polynomial of the fifth degree, the van der Pol equation has the form

$$\ddot{x} - \epsilon(1 + \alpha x^2 - \beta x^4)\dot{x} + x = 0. \tag{4.2}$$

Using the preceding procedure one gets

$$\frac{d\rho}{d\theta} = -2\rho[\epsilon(\,)\,\mathrm{Sin}^2\theta + \epsilon^2(\,)^2\,\mathrm{Sin}^3\theta\,\mathrm{Cos}\,\theta + \epsilon^3(\,)^3\,\mathrm{Sin}^4\theta\,\mathrm{Cos}^2\theta + \cdots],$$

where $(\,) = (1 + \alpha\rho\,\mathrm{Cos}^2\theta - \beta\rho^2\,\mathrm{Cos}^4\theta)$. The perturbation method limited to the zero, and the first approximation gives

$$\rho_0 = K_0 = \mathrm{Const};$$

$$\rho_1 = -2[\rho_0 \int \mathrm{Sin}^2\theta d\theta + \alpha\rho_0^2 \int \mathrm{Cos}^2\theta\,\mathrm{Sin}^2\theta d\theta - \beta\rho_0^3 \int \mathrm{Cos}^4\theta\,\mathrm{Sin}^2\theta d\theta] + K_1$$

and the elimination of the secular term gives

$$\rho_0 = \alpha/\beta + \sqrt{(\alpha/\beta)^2 + (8/\beta)},$$

so that, up to the terms of the order ϵ^2 one gets

$$\rho = \rho_0 + \epsilon\rho_1 = \rho_0 - \epsilon\left[\frac{1}{2}\left(\rho_0 + \frac{1}{64}\beta\rho_0^3\right)\mathrm{Sin}\,2\theta + \right.$$

$$\left. + \frac{1}{16}\rho_0^2\left(\alpha - \frac{1}{2}\beta\right)\mathrm{Sin}\,4\theta - \frac{1}{96}\beta\rho_0^3\,\mathrm{Sin}\,6\theta\right] + K_2.$$

There exists obviously no ρ_0 for $\beta = 0$ since the damping term is then negative for all values of x. For $\alpha = 0$, $\beta = 1$, (4.2) becomes

$$\ddot{x} - \epsilon(1 - x^4)\dot{x} + x = 0, \tag{4.5}$$

in which case

$$\rho_0 = 2\sqrt{2}.$$

Interesting cases arise when the form of the van der Pol equation for an electron tube oscillator is modified by the presence of certain

variable conductors in the oscillating circuit. We shall consider one such case in connection with the circuit shown in Fig. 1. If all parameters (L, C and R) are constant, it is well known (5) that the van der Pol equation in this case is of the form

$$\frac{d^2\nu}{d\tau^2} - (\beta + 2\gamma\nu - 3\delta\nu^2)\frac{d\nu}{d\tau} + \nu = 0, \tag{4.6}$$

where $\nu = \nu_g/\nu_s$ is a dimensionless variable (ν_g is the grid voltage; ν_s the

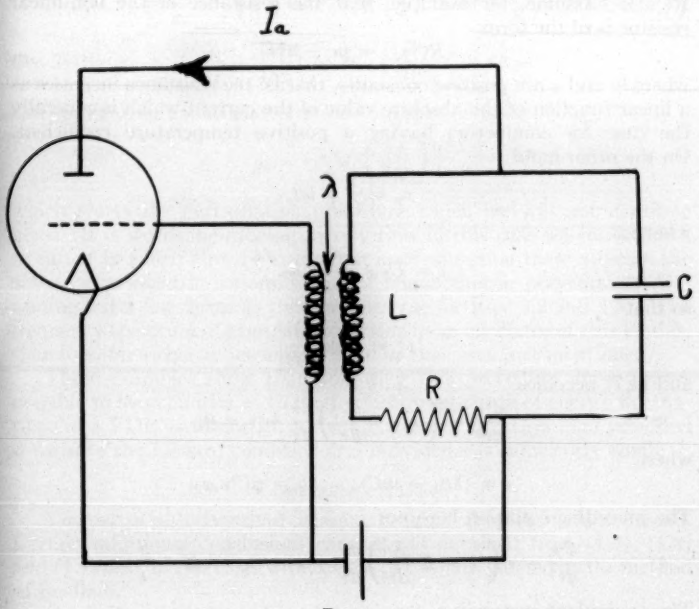

FIG. 1.

constant "saturation voltage"), $\tau = \omega_0 t$; $\omega_0 = \sqrt{1/LC}$; $\beta = (\lambda\beta_1 - RC)\omega_0$

$\gamma = \lambda\gamma_1\omega_0$; $\quad \delta = \lambda\delta_1\omega_0$; $\quad \beta_1 = S_1$; $\quad \gamma_1 = S_2\nu_s$; $\quad \delta_1 = -S_3\nu_s^2$,

and the non-linear function, the anode current, is assumed to be represented by the polynomial

$$I_a = \phi(\nu_g) = I_0 + S_1\nu_g + S_2\nu_g^2 + S_3\nu_g^3.$$

Let us modify the problem by replacing the constant resistor R by a variable one $R(|i|)$, depending on the absolute value of the current and

assume, moreover, that the non-linearity of $R(|i|)$ appears *before* the non-linearity of the electron tube is felt. In other words, we wish to consider the case when the electron tube operates still on the rectilinear part of its characteristic (that is, $\gamma = \delta \cong 0$). Equation 4.6 in such a case becomes

$$\frac{d^2v}{d\tau^2} - [\lambda\beta_1 - R(|i|)C]\frac{dv}{d\tau} + v = 0. \tag{4.7}$$

It is necessary to make a certain assumption regarding the function $R(|i|)$. Assume, for example, that the resistance of the non-linear resistor is of the form

$$R(|i|) = m + n|i|,$$

where m and n are positive constants, that is, the resistance increases as a linear function of the absolute value of the current which is generally the case for conductors having a positive temperature coefficient. On the other hand

$$v_g = \frac{1}{C}\int i dt,$$

whence

$$i = Cv_s\dot{v} = Cv_s\omega_0\frac{dv}{d\tau}$$

so that

$$|i| = Cv_s\omega_0\left|\frac{dv}{d\tau}\right|$$

and (4.7) becomes

$$\frac{d^2v}{d\tau^2} - \left(\epsilon - b\left|\frac{dv}{d\tau}\right|\right)\frac{dv}{d\tau} + v = 0,$$

where

$$\epsilon = (\lambda\beta_1 - mC); \qquad b = nC^2v_s\omega_0.$$

The preceding equation becomes

$$\frac{d^2v}{d\tau^2} - \epsilon\left(1 - K\left|\frac{dv}{d\tau}\right|\right)\frac{dv}{d\tau} + v = 0, \qquad K = \frac{b}{\epsilon}.$$

The equivalent system is

$$\frac{dv}{d\tau} = y; \qquad \frac{dy}{d\tau} = \epsilon(1 - K|y|)y - v.$$

Assuming that ϵ and τ are small, Eq. 1.9 in this case is

$$\frac{d\rho}{d\theta} = \frac{2\epsilon(\ )\rho\,\mathrm{Sin}^2\,\theta}{\epsilon(\ )\,\mathrm{Sin}\,\theta\,\mathrm{Cos}\,\theta - 1}$$

$$= -2\rho[\epsilon(\ )\,\mathrm{Sin}^2\,\theta + \epsilon^2(\ )^2\,\mathrm{Sin}^3\,\theta\,\mathrm{Cos}\,\theta + \epsilon^3(\ )^3\,\mathrm{Sin}^4\,\theta\,\mathrm{Cos}^2\,\theta + \cdots],$$

where

$$(\ ) = (1 - K\tau|\mathrm{Sin}\,\theta|) = (1 - K\rho^3|\mathrm{Sin}\,\theta|).$$

The perturbation method gives

$$\frac{d\rho_0}{d\theta} = 0; \qquad \rho_0 = K_0 = \text{Const.}$$

$$\frac{d\rho_1}{d\theta} = -2(1 - K\rho_0^{\frac{1}{2}}|\text{Sin }\theta|)\rho_0 \text{Sin}^2\theta =$$

$$= -\rho_0 + \rho_0 \text{Cos } 2\theta + K\rho_0^{\frac{1}{2}}(|\text{Sin }\theta| - \text{Cos } 2\theta|\text{Sin }\theta|).$$

Replacing

$$|\text{Sin }\theta| = \frac{2}{\pi} - \frac{4}{\pi}\left(\frac{1}{1.3}\text{Cos } 2\theta + \frac{1}{3.5}\text{Cos } 4\theta + \frac{1}{5.7}\text{Cos } 6\theta + \cdots\right)$$

$$\text{Cos } 2\theta|\text{Sin }\theta| = -\frac{2}{3\pi} + \frac{28}{15\pi}\text{Cos } 2\theta - \frac{76}{105\pi}\text{Cos } 4\theta - \cdots$$

and eliminating the secular term one obtains

$$\rho_0 = r_0^2 = \left(\frac{3\pi}{8K}\right)^2,$$

which starts the perturbation procedure which we will not continue here. It is worth mentioning merely that in this case we encounter a situation in which already in the first approximation there appears the whole trigonometric series instead of trigonometric polynomials containing but a few terms as this was the case for Eqs. 1.2 and 4.5. The frequency spectrum of energy fluctuations in an oscillator of this kind is, therefore, far richer in harmonics than in the cases just mentioned.

These examples show that, following this procedure, it is always possible to form an idea as to the frequency spectrum of energy fluctuations in a VDP oscillator for a given non-linear function $F(x)$ provided it satisfies the Liénard condition and provided ϵ is sufficiently small.

5. CASE WHEN ϵ IS LARGE

The perturbation method ceases to be applicable when ϵ is not small. Certain additional conclusions can be still obtained from (1.7), (1.8) and (1.9) also, in this case, with the aid of the data yielded by the method of isoclines.

It is to be noted that the maxima and minima of both polar curves $\rho(\theta)$ and $r(\theta)$ are situated on the same radii-vectors since the $\rho(\theta)$ curve is obtained merely by squaring the radii vectors of the $r(\theta)$ curve for each θ and, conversely if $\rho(\theta)$ curve is given, the $r(\theta)$ curve can be obtained by an inverse operation. We shall speak preferably of the energy curve $\rho(\theta)$ inasmuch as in this manner it will be possible to derive certain physical conclusions regarding the VDP oscillator but occasionally we shall refer also to the integral curve $r(\theta)$ in view of the above relation between these two closed curves.

From (1.7) it follows that the maxima and minima of energy occur when $\rho(\theta) = 1/\text{Cos}^2\theta$ which in cartesian coordinates is obviously $x = \pm 1$.

For these particular values of θ the term with $\dot{x}$ in (1.2) vanishes and the VDP oscillator coincides instantaneously with the harmonic oscillator of this particular (ρ_{max} or ρ_{min}) energy content. One can also verify this circumstance by replacing $\rho = 1/\mathrm{Cos}^2\,\theta$ in (1.8) which gives $\dot{\theta} = -1$ which in conjunction with the condition $\dot{\rho} = 0$ gives conditions (1.5) for a harmonic oscillator. In order to distinguish maxima from minima it is sufficient to calculate $\ddot{\rho}$ which gives

$$\ddot{\rho} = 2\epsilon[\dot{\rho}(\mathrm{Sin}^2\,\theta - 2\rho\,\mathrm{Sin}^2\,\theta\,\mathrm{Cos}^2\,\theta) + 2\rho\dot{\theta}(\mathrm{Sin}\,\theta\,\mathrm{Cos}\,\theta + \rho\,\mathrm{Sin}^3\,\theta\,\mathrm{Cos}\,\theta - \rho\,\mathrm{Sin}\,\theta\,\mathrm{Cos}^3\,\theta)].$$

Replacing in this, expressions $\dot{\rho} = 0$, $\dot{\theta} = -1$, $\rho = 1/\mathrm{Cos}^2\,\theta$, one finds

$$\ddot{\rho} = -4\epsilon\,\mathrm{Tan}^2\,\theta,$$

which shows that the maxima of energy are located in the first and the third quadrants of the polar curve $\rho(\theta)$ and minima in the second and in the fourth quadrants which also agrees with the data yielded by the method of isoclines. Similarly, when ϵ increases the isocline method shows that the maxima increase and the minima decrease but since the condition $\rho\,\mathrm{Cos}^2\,\theta = 1$ is independent of ϵ, it is clear that the values of θ corresponding to ρ_{max} approach the y axis and those for ρ_{min} recede to the x axis while still being in their respective quadrants. This also agrees with the data furnished by the isocline method. There exists thus a definite relation between the magnitude of the maxima and minima of energy and their phase in the polar curve.

For a sufficiently large ϵ and in the neighborhood of maxima of the energy content, the rate of change of energy $\dot{\rho}$ varies very rapidly even for a small variation $\Delta\theta$ around the value $\theta = \theta_{max}$. Thus, for instance, from the isocline curve for $\epsilon = 30$, $\rho_{max} \cong 1300$ and $\theta_{max} \cong 88.4°$. For $\Delta\theta = \pm 0.1°$, $\dot{\rho}$ changes from about -13000 (for $\Delta\theta = -0.1°$) to about $+11000$ (for $\Delta\theta = +0.1°$) in the dimensionless units used here, whereas in the neighborhood of minima the same variation $\Delta\theta$ accounts for a small part of one per cent of the above variation. If one wishes to give a physical analogue of the behavior of the VDP oscillator in the neighborhood of its maxima energy points, at least as far as energy fluctuations are concerned, perhaps a pneumatic hammer or a similar device may give an adequate analogy. In fact in a device of this kind a rapid acceleration of the hammer with the incident increase in its energy content (which is the kinetic energy here) is followed by a not less rapid deceleration when the hammer strikes an energy absorbing medium and thus loses its energy.

In addition to one maximum and one minimum of energy per one half cycle (the other half cycle being identical) the VDP oscillator has also one *stationary* point for $\theta = 0$ (for the other half-cycle this stationary point occurs for $\theta = \pi$) at which the energy passes through a stationary value without being either maximum or minimum. One sees

this from (1.7) which shows that $\dot{\rho}$ passes through zero at these points without changing its sign. One notes also that $\ddot{\rho} = 0$ at this point. When ϵ is large these stationary points are close to the minima points of energy. The investigation of the behavior of an integral curve in the neighborhood of these stationary points is far from being simple, if ϵ

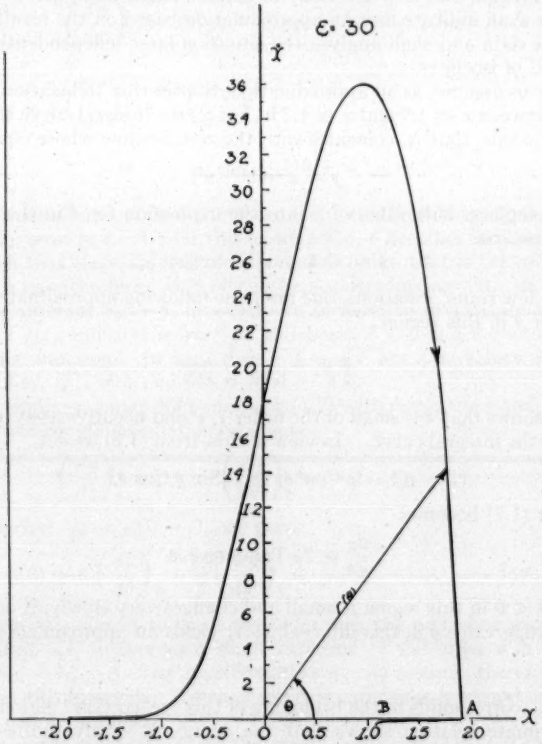

FIG. 2.

is large enough and this is probably one of the principal difficulties of the van der Pol equation. The method of isoclines shows, in fact, that there is a sharp bend of integral curves in this "relaxation region" as can be seen from Fig. 2, representing the integral curve $r(\theta)$ for $\epsilon = 30$ constructed by the method of isoclines.[3] If one follows this integral curve

[3] The author is indebted to Miss E. Yost for this construction.

in the positive direction (that is, clockwise) one finds that it cuts the x-axis at right angles (point A) but immediately after that the integral curve has an almost 90° bend and follows practically the x-axis toward the origin. The accuracy of the graphical construction is obviously insufficient to be able to specify the details of what happens in this critical region and it is necessary to make a closer analysis.

We shall indicate first an approximation based on the results of the isocline data and shall analyze the situation later independently of the method of isoclines.

Let us assume, as an approximation, that in this "relaxation region" (say between $x \cong 1.9$ and $x \cong 1.2$ in Fig. 2) the integral curve is parallel to the x-axis, that is, coincides with the zero isocline whose equation is

$$y = x/\epsilon(1 - x^2).$$

If one replaces this value of y into the expression for $\dot{\theta}$ in the x, y coordinates, *viz:*

$$\dot{\theta} = -1 + \epsilon(1 - x^2)xy/\rho,$$

after a few transformations, one finds the following approximate expression for $\dot{\theta}$ in this region

$$\dot{\theta} = -\frac{1}{\epsilon^2(1 - x^2)^2},$$

which shows that $\dot{\theta}$ is small of the order $1/\epsilon^2$ and negative as everywhere else on the integral curve. In view of this, from (1.8) we get

$$\epsilon(1 - \rho \operatorname{Cos}^2 \theta) \cong 1/\operatorname{Sin} \theta \operatorname{Cos} \theta,$$

so that (1.7) becomes

$$\frac{d\rho}{d\theta} \cong 2\rho \operatorname{Tan} \theta \cong 2\rho\theta. \tag{5.1}$$

Since $\theta < 0$ in this region is small and changes very slowly, if one takes its average value $\bar{\theta}$ in this interval, (5.1) yields an approximate formula

$$\rho = \rho_0 e^{2\bar{\theta}t} \tag{5.2}$$

where ρ_0 corresponds to the beginning of this "relaxation" region. This approximate relation shows that the energy is slowly drained away from the system in a manner in which the electrostatic energy of a charged condenser disappears gradually owing to an imperfect dielectric.

This somewhat crude analysis is merely a physical interpretation of the results yielded by the method of isoclines.

For that reason it is preferable to investigate the behavior of the functions $\dot{\rho}(\theta)$ and $\dot{\theta}(\theta)$ in a small interval $(\theta_1, -\theta_1)$; $\theta_1 > 0$ around $\theta = 0$ (the argument applies also to $\theta = \pi$). This will permit obtaining certain conclusions directly without relying on the method of isoclines.

Differentiating (1.8) with respect to θ and setting $\theta = 0$ after the differentiation one gets

$$\left(\frac{d\dot\theta}{d\theta}\right)_0 = -\epsilon(\rho_0 - 1); \qquad \left(\frac{d^2\dot\theta}{d\theta^2}\right)_0 = 0;$$

$$\left(\frac{d^3\dot\theta}{d\theta^3}\right)_0 = \epsilon(10\rho_0 - 4) \text{ etc.}, \qquad \rho_0 = \rho(0),$$

so that

$$\dot\theta(\theta) = \dot\theta_0 + \theta\left(\frac{d\dot\theta}{d\theta}\right)_0 + \frac{\theta^2}{2}\left(\frac{d^2\dot\theta}{d\theta^2}\right)_0 + \cdots$$

$$= -1 - \epsilon(\rho_0 - 1)\theta + \epsilon(5\rho_0 - 2)\frac{\theta^3}{3} + \cdots. \quad (5.3)$$

Since θ is small and ρ_0 is of the order 4 one can limit this expansion to the linear term in θ. Under this assumption, $\dot\theta$ becomes very small for $\theta < 0$ such that $\epsilon(\rho_0 - 1)|\theta|$ is of the order of unity, that is $|\theta| \cong 0(1/3\epsilon)$. In such a case the term with $\epsilon\theta^3$ can be neglected as we did. If, therefore, the interval θ_1, $-\theta_1$ in which we propose to investigate the behavior of $\dot\rho(\theta)$ and $\dot\theta(\theta)$ is fixed on this basis, $\theta < 0$ is a monotonically increasing function. In fact $\dot\theta = -1 - K\theta$ has the values $|\dot\theta|_{\theta_1} = 1 + K\theta_1$; $|\dot\theta|_0 = 1$ and $|\dot\theta|_{-\theta_1} = 1 - K\theta_1$.

In a similar manner differentiating (1.7) with respect to θ and setting $\theta = 0$ after the differentiation, one gets

$$\left(\frac{d\dot\rho}{d\theta}\right)_0 = 0; \qquad \left(\frac{d^2\dot\rho}{d\theta^2}\right)_0 = -2\epsilon\rho_0(\rho_0 - 1).$$

As, moreover, $\dot\rho_0 = \dot\rho(0) = 0$, one gets

$$\dot\rho(\theta) = \dot\rho(0) + \theta\left(\frac{d\dot\rho}{d\theta}\right)_0 + \frac{\theta^2}{2}\left(\frac{d^2\dot\rho}{d\theta^2}\right)_0 + \cdots \cong -2\epsilon\rho_0(\rho_0 - 1)\theta^2. \quad (5.4)$$

Since $\epsilon|\theta|$ is assumed to be of the order one, the preceding expression shows that $\dot\rho(\theta)$ undergoes a small variation of the order θ in the interval $(\theta_1, -\theta_1)$. As first approximation we can assume, therefore that $\rho \cong \rho_0$ in this interval. We shall indicate later how a second approximation can be obtained.

It is useful now to specify the interval $(\theta_1, -\theta_1)$, $\theta_1 > 0$ in which the preceding assumptions apply. In the construction of the curve of Fig. 2, $\epsilon = 30$ was assumed which is a purely arbitrary value selected with a view to go a little beyond the value ($\epsilon = 10$) which van der Pol used in his construction. This permits obtaining a more pronounced "relaxation region" between the points A and B. On the other hand, van der Pol, in his analysis of a relaxation oscillation circuit with constants commonly encountered in applications, finds $\epsilon \cong 3.10^5$, that is $K \cong 10^6$. This gives the value of $\theta < 0$, for which $\dot\theta$ becomes very

small, of the order of 1 sec. of arc. This means that the motion of the representative point which is practically tangential (with respect to the radius vector) for $\theta = 0$, becomes radial for $\theta \cong -1$ sec., which gives an idea as to the order of magnitude of the interval $(\theta_1, -\theta_1)$ in question for the various values of ϵ.

As regards the function $\dot{\rho}(\theta)$, (5.4) shows that, under the assumed approximation, it is an even function of θ; moreover $\dot{\rho}(\theta)$ is negative in this interval, that is, the energy decreases between θ_1, and $-\theta_1$.

We propose now to calculate the loss of energy $-\Delta\rho_1$, and $-\Delta\rho_2$ in the half-intervals $(\theta_1, 0)$ and $(0, -\theta_1)$, respectively, when the radius vector traverses the small arc $(\theta_1, -\theta_1)$. One has

$$-\Delta\rho_1 = \int_{\theta_1}^{0} \dot{\rho} dt; \qquad -\Delta\rho_2 = \int_{0}^{-\theta_1} \dot{\rho} dt.$$

From (5.3) and (5.4) we have

$$\dot{\theta} = -(1 + K\theta); \qquad \dot{\rho} = -2\rho_0 K\theta^2,$$

where $K = \epsilon(\rho_0 - 1)$. Thus

$$\dot{\rho} dt = 2\rho_0 K \frac{\theta^2}{1 + K\theta} d\theta$$

and, therefore,

$$-\Delta\rho_1 = 2\rho_0 K \int_{\theta_1}^{0} \frac{\theta^2}{1 + K\theta} d\theta; \qquad -\Delta\rho_2 = 2\rho_0 K \int_{0}^{-\theta_1} \frac{\theta^2}{1 + K\theta} d\theta.$$

Under this assumption

$$-\Delta\rho_1 = -\frac{2\rho_0}{K^2}\left[\tfrac{1}{2}(1 + K\theta_1)^2 - 2(1 + K\theta_1) + \ln(1 + K\theta_1) + \tfrac{3}{2}\right], \quad (5.5)$$

$$-\Delta\rho_2 = \frac{2\rho_0}{K^2}\left[\tfrac{1}{2}(1 - K\theta_1)^2 - 2(1 - K\theta_1) + \ln(1 - K\theta_1) + \tfrac{3}{2}\right]. \quad (5.6)$$

Since in the half-interval $(0, -\theta_1)$ the quantity $1 - K\theta_1 > 0$ becomes very small, $\ln(1 - K\theta_1)$ is a very large negative number so that $\Delta\rho_2 \gg \Delta\rho_1$. On the other hand, since $-\Delta\rho_1$ and $-\Delta\rho_2$ represent the decrease of the radius vector in $(\theta_1, 0)$ and $(0, -\theta_1)$, respectively, one obtains a situation depicted in Fig. 3 which explains the origin of a sharp bend in the curve of energy $\rho(\theta)$ (and also the integral curve $r(\theta)$) in the negative neighborhood ($\theta < 0$) of the stationary point A. Once the dissymmetry of $\dot{\theta}(\theta)$ has been ascertained starting from the assumption that $\rho \cong \rho_0$ in this angular interval $(\theta_1, -\theta_1)$, it is possible to carry out the second approximation using, for example, the values $\rho_0 + \Delta\rho_1/2$, $\rho_0 - \Delta\rho_2/2$ instead of ρ_0 (and the corresponding values K_1 and K_2) in both half-intervals which gives a more correct estimate for $\Delta\rho_1$ and $\Delta\rho_2$ and thus calculate the shape of the $\rho(\theta)$ curves in this neighborhood.

The sharp bend of the curves $\rho(\theta)$ and $r(\theta)$ is thus due to a very marked assymmetry of the function $\dot{\theta}(\theta)$ in this region while the function $\dot{\rho}(\theta)$ remains symmetrical about these stationary points. From a physical standpoint this circumstance means that, on account of a smaller velocity $\dot{\theta}$ in the $(0, -\theta_1)$ half interval the same drain of energy (for the same θ) persists for a longer time in the negative half interval than in the positive one which is traversed rapidly, so that the actual decrease of energy is greater in $(0, -\theta_1)$ than in $(\theta_1, 0)$. It must be noted that for very large values of ϵ, like those mentioned by van der Pol, the bend of integral curves becomes so sharp that the analyticity of the curve in this region is bad. For that reason the Taylor expansion in this region becomes rather complicated as compared to the remaining portions of the curve. It is likely that these *local* complications in the

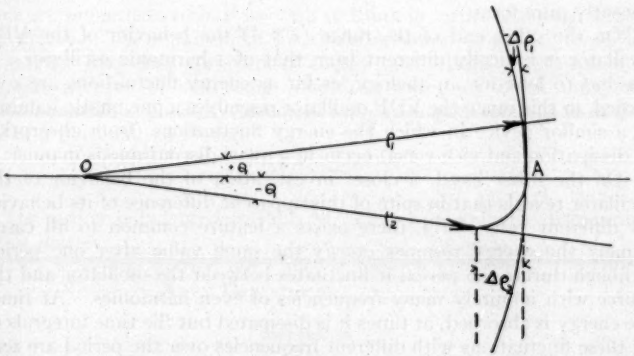

FIG. 3.

analytical structure of the integral curve at the beginning of this "relaxation" region, is the main reason why no explicit solution of the van der Pol equation (for example, in the form of a series) could be found as yet, in spite of nearly twenty years of effort, although considerable progress has recently been accomplished in connection with a qualitative analysis of this difficult problem (6).

CONCLUDING REMARKS

The most interesting feature of the VDP oscillator is the fact that its behavior is widely different for different values of the parameter ϵ.

At one end of the range ($\epsilon \ll 1$) the VDP oscillator differs very little from the harmonic oscillator and thus offers practically a perfect physical image of the latter. Probably it is not an exaggeration to say that, since the time of Galileo who introduced the concept of the

harmonic oscillator, we were able to actually observe a practically perfect physical image of the latter only when the VDP oscillator became available relatively a short time ago. In fact, very likely, there exists no better physical image of a simple harmonic motion than that which is produced by modern high quality electron tube oscillators, particularly those whose frequency is stabilized by quartz units. But this almost perfect physical image contains a germ of an immense complexity due to the presence of an infinite spectrum of frequencies with which the energy fluctuates between the oscillator and the source of energy. These fluctuations escape our observation, however, if ϵ is very small and, as the result of this, what is actually observed is only the constant term in the infinite array of terms (2.7). However, it is precisely this hidden complexity of vanishingly small energy fluctuations which permits obtaining a simple harmonic oscillation in its apparently pure form.

On the other end of the range ($\epsilon \gg 1$) the behavior of the VDP oscillator is radically different from that of a harmonic oscillator. If one has to look for an analogy, as far as energy fluctuations are concerned, in this range the VDP oscillator resembles a pneumatic hammer or a similar device in which the energy fluctuations (from absorption to dissipation and vice versa) occur in a quasi-discontinuous manner.

On the other hand, a closer investigation of the behavior of the oscillator reveals that in spite of this apparent difference of its behavior for different values of ϵ, there exists a feature common to all cases, namely the energy resumes *exactly* the same value after one period although during the period it fluctuates between the oscillator and the source with infinitely many frequencies of even harmonics. At times the energy is absorbed, at times it is dissipated but the time integrals of all these fluctuations with different frequencies over the period are zero and there remains only the average constant term around which these fluctuations occur. If these fluctuations are vanishingly small in comparison with the constant energy content of the VDP oscillator, it behaves approximately as a conservative system. If $\epsilon \gg 1$, on the contrary, the fluctuations of energy dominate everything else to such an extent that it becomes even impossible to answer the question: around which average constant value of energy do these fluctuations occur?

In addition to these fluctuations of energy, there exist also fluctuations in the angular velocity of the radius vector of the representative point moving on the integral curve. If ϵ is small enough these fluctuations are also small so that, from this standpoint, the motion on integral curves does not differ much from the corresponding motion for the harmonic oscillator in which case these fluctuations are rigorously zero. For an increasing ϵ these fluctuations in angular velocity become more and more pronounced and, for very large values of ϵ, the angular velocity becomes of the order $1/\epsilon^3$, that is very small, in the neighborhood of the

points at which the energy passes through a stationary value. In this neighborhood one observes the interesting phenomenon of a "relaxational" drain of energy from the system and results in a sharp bend in the integral curve.

In spite of a number of common features between a harmonic, and a VDP oscillator for $\epsilon \ll 1$, there exists a fundamental difference between the two oscillators, namely: a harmonic oscillator can oscillate with *any* energy content prescribed by the initial conditions, whereas the energy content of a VDP oscillator does not depend at all on these conditions. In fact, the oscillator "selects" so to speak its own energy content consistent with the form of the non-linear function $F(x)$ as well as with the parameters of the system. This remarkable peculiarity of the VDP oscillator, as we saw, is due to the fact that a stationary periodic motion in this case is possible only in the case when *all* secular terms are reduced to zero, if we wish to think in terms of the perturbation theory. The requirement for the elimination of secular terms in the infinite frequency spectrum of energy fluctuations thus imposes a requisite number of additional conditions owing to which only *one* periodic motion is possible, instead of infinity of such motions as in the case of a harmonic oscillator.

Acknowledgments

The author is indebted to Prof. M. Schiffer for valuable discussions of this matter.

This work was carried out under a research program of the Office of Naval Research, Navy Department.

REFERENCES

(1) BALTH. VAN DER POL, "On Relaxation Oscillations," *Phil. Mag.*, Vol. 27 (1926).
—— "Oscillations Sinusoidales et de Relaxation," *l'Onde Electrique*, Vol. 9 (1930).
—— "The Non-Linear Theory of Electrical Oscillations," *Proc. IRE*, Vol. 22 (1934).
(2) A. LIÉNARD, "Etude des Oscillations Entretenues," *Revue Générale de l'Electricité*, Vol. 23 (1928).
(3) E. AND H. CARTAN, "Note sur la Génération des Oscillations Entretenues," *Ann des P. T. T.*, Vol. 12 (1925).
(4) N. LEVINSON AND O. K. SMITH, "A General Equation for Relaxation Oscillations," *Duke Math. Jour.*, Vol. 9 (1942).
(5) A. ANDRONOW AND S. CHAIKIN, "Theory of Oscillations," Chapter VII, Moscow (1937); English language edition of this book will appear shortly in Princeton Univ. Press.
(6) D. FLANDERS AND J. STOKER, "The Limit Case of Relaxation Oscillations," New York University (1946).
J. LA SALLE, "Relaxation Oscillations" (to appear shortly).

New Etching Process.—A revolutionary new etching process to prepare metal surfaces for microscopic examination and photography has been developed by the Ford Motor Company.

The unique metal-etching method—never before used in industry—utilizes ionized atoms. The process is known as cathodic vacuum etching.

Etching is widely used in industry to examine metal structures for determining quality and aiding in development of new materials or manufacturing processes.

Cathodic vacuum etching has brought an important improvement. It enables the taking of an unusually clear photograph of flow lines—a curious strata-like pattern which indicates the direction the metal flowed when forged under high pressure.

The new etching technique works this way: The metal sample is placed in a partial vacuum with argon, a rare gas found in the air. Twelve thousand volts of electricity are charged into the vacuum, creating argon ions which bombard the metal surface and knock off minute particles.

Under the newly developed method the physical features of metal can be examined under a microscope and measured accurately as to their effect on strength and performance in whatever part of the Ford cars the metal ultimately will become a fixture.

Flow lines in steel samples previously undetected now have been revealed by cathodic bombardment.

Comparison of the structure pattern produced by the best chemical etching method revealed that the new cathodic treatment brings out the true microstructure of the metal with greater detail and clarity.

A special pressure-rolled Ford front wheel spindle was examined experimentally by the usual microscopic technique. No superficial layer of flowed metal could be detected by the chemical etching process. However, cathodic bombardment etching revealed the entire superficially rolled structure, showing individual flow lines which indicated that deformation was only .005-inch deep.

Results also were obtained which indicate that grain structure of metals also can be more clearly shown by cathodic bombardment. Ford engineers have begun an extensive program to explore this phase of cathodic etching.

Photographs illustrating cathodic etched structures were awarded first prize in an exhibition sponsored by the American Society for Metals.

MINIMUM AND MAXIMUM SENSITIVITIES OF PHOTOGRAPHIC EMULSIONS *

BY

A. P. H. TRIVELLI [1]

INTRODUCTION

In 1940, Bruscaglioni (1)[2] investigated the minimum sensitivity of photographic plates by measuring the quantic absorption of the incident radiation. The present author has investigated the same problem by means of Silberstein and the author's quantum theory of exposure (2), which is an extension of Silberstein's original theory (3). The original theory was restricted to the study of 1-quantum grains, which are grains made developable by the effective absorption of one quantum, spread out in one layer on a flat surface. It was advisable to start with 1-quantum grains because the differences between the sensitivities measured by the wave theory and those determined by the quantum theory could be expected to be more pronounced with the one-quantic than with the many-quantic hypothesis of sensitivity. The only experimental evidence obtained, however, was found with X-ray exposures (4).

Because the measurements made with one-grain-layer coatings of experimental and commercial emulsions cannot be compared with the measurements made with multi-grain-layer coatings of these emulsions, the theory was extended so that the sensitivity of multi-grain-layer coatings could be measured, and the quantic sensitivity, r, be determined from 1 to ∞. The quantic sensitivity, r, denotes the minimum number of absorbed quanta required to make a grain developable. These quanta are called the "effective" quanta.

Definite indications of a minimum sensitivity were obtained empirically for certain groups of photographic materials. A general discussion will also be given of the conditions for approaching a maximum sensitivity of photographic emulsions.

THE EFFECTIVE SENSITIVITY

In the quantum theory of exposure, the sensitivity of a grain is defined as its probability (p) of becoming developable by the absorption of at least r quanta. From the beginning, p has represented the probability that a single grain of size, a, will absorb effectively a single quantum projected upon a plate coated with one layer of grains. This probability is written ϵa. No new assumption was introduced in the

* Communication No. 1243 from the Kodak Research Laboratories.

[1] Kodak Research Laboratories, Eastman Kodak Company, Rochester, N. Y.

[2] The boldface numbers in parentheses refer to the references appended to this paper.

theory by this expression; the probability per unit projective area of the grain was merely denoted by ϵ. It was not assumed that ϵ was dependent upon the grain size, a.

It is clear that ϵ/r represents the probability of a single grain of size, a, becoming developable per quantum effectively absorbed. This holds true for single grains and also for an assemblage of grains of average grain size, $\bar{a}$, having constant r- and constant ϵ-values (5).

Quantic sensitivity measurements of a number of experimental photographic emulsions have shown that their fog-corrected characteristic curves can be represented by single-term or double-term equations. The single-term equation (2) is given by the general expression

$$D(y) = D_{max}F(y), \tag{1}$$

in which D, D_{max}, and y represent density, maximum density, and exposure, respectively.

THE MINIMUM SENSITIVITY

The first data investigated consisted of forty-two fog-corrected single-term characteristic curves of pure silver bromide emulsions, chosen at random from converted and non-converted, unsensitized and sensitized emulsions, developed in different developers for different times. The sensitivity constants ranged from $\epsilon/r \times 10^4 = 0.9$ to 14.4, and, correspondingly, from $10/i = 1.2$ to 280.0, in which i is the inertia point of the $D/\log E$ curve and $10/i$ the well-known inertia speed of photographic materials. The Bravais-Pearson correlation coefficient, k, between the ϵ/r- and $10/i$-values was found to be equal to 1.0. The linear equation which was calculated by the method of least squares in terms of $x = 10/i$ and $y = \epsilon/r \times 10^4$ is:

$$y = 0.0521x + 0.6,$$

which gives

$$[\epsilon/r]_{min} = 6 \times 10^{-5}.$$

A similar investigation was carried out with the fog-corrected characteristic curves of experimental silver bromoiodide emulsions containing 2.56 moles per cent of silver iodide which were representable by the same general equation (1). However, only a few emulsions of this type were available; not more than eleven curves could be collected. The sensitivity measurements ranged from $\epsilon/r \times 10^4 = 0.28$ to 11.70, and correspondingly, from $10/i = 6.2$ to 580.0. The correlation coefficient for $x = 10/i$ and $y = \epsilon/r \times 10^4$ is also 1.0. The linear relationship which was calculated by the method of least squares is:

$$y = 0.0207x + 0.4,$$

which gives

$$[\epsilon/r]_{min} = 4 \times 10^{-5}.$$

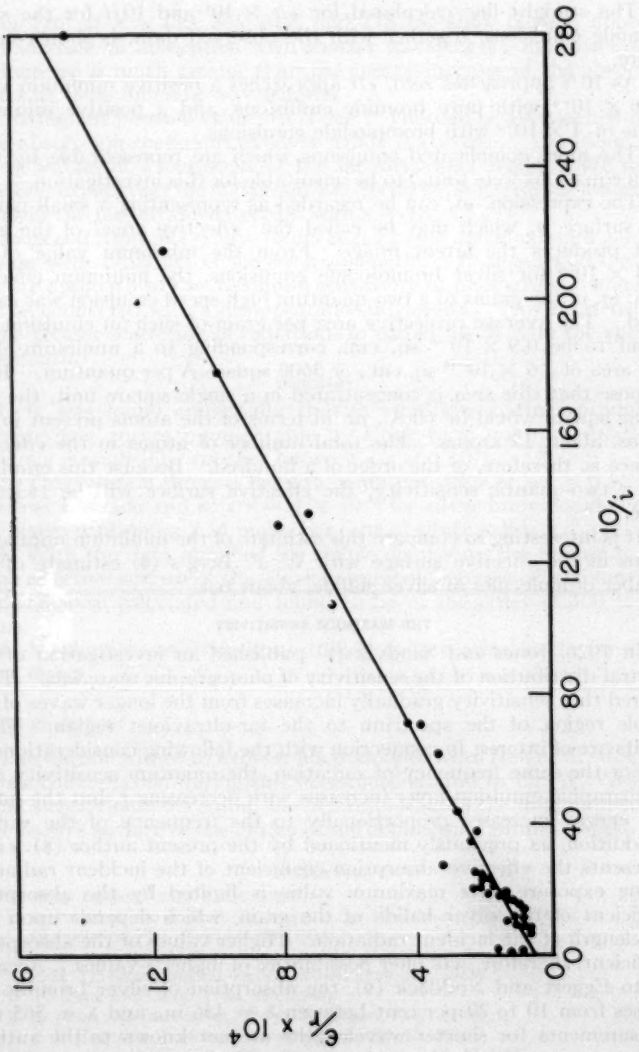
280
240
200
160
120
80
40
0
10/i
16
12
8
4
0
ε/t x 10⁴

The straight line calculated for $\epsilon/\tau \times 10^4$ and $10/i$ for the silver bromide emulsions, together with the observed data, is shown in the figure.

As $10/i$ approaches zero, ϵ/τ approaches a positive minimum value of 6×10^{-5} with pure bromide emulsions, and a positive minimum value of 4×10^{-5} with bromoiodide emulsions.

The more complicated emulsions which are representable by two-term equations were found to be unsuitable for this investigation.

The expression, ϵa, can be regarded as representing a small part of the surface, a, which may be called the "effective area" of the grain that produces the latent image. From the minimum value of $\epsilon/\tau = 4 \times 10^{-5}$ for silver bromoiodide emulsions, the minimum effective area, ϵa, of the grains of a two-quantum high-speed emulsion was calculated. The average projective area per grain of such an emulsion was found to be 0.9×10^{-8} sq. cm., corresponding to a minimum effective area of 3.6×10^{-13} sq. cm., or 3600 square Å per quantum. If we suppose that this area is concentrated in a single square unit, the side of the square would be 60 Å., or, in terms of the atoms present in the grains, about 12 atoms. The total number of atoms in the effective surface is, therefore, of the order of a hundred. Because this emulsion has a two-quantic sensitivity, the effective surface will be twice as large.

It is interesting to compare this estimate of the minimum number of atoms in the effective surface with W. F. Berg's (6) estimate of the number of molecules of silver sulfide, about ten.

THE MAXIMUM SENSITIVITY

In 1926, Jones and Sandvik (7) published an investigation of the spectral distribution of the sensitivity of photographic materials. They showed that sensitivity gradually increases from the longer waves of the visible region of the spectrum to the far-ultraviolet region. These results are of interest in connection with the following considerations.

For the same frequency of radiation, the quantum sensitivity of a photographic emulsion layer increases with decreasing τ, but the quantum energy increases proportionally to the frequency of the waves. In addition, as previously mentioned by the present author (8), ϵ also represents the effective absorption coefficient of the incident radiation during exposure. Its maximum value is limited by the absorption coefficient of the silver halide of the grain, which depends upon the wavelength of the incident radiation. Higher values of the absorption coefficient, therefore, will offer possibilities of higher ϵ-values. According to Eggert and Noddack (9), the absorption of silver bromide increases from 10 to 20 per cent between $\lambda = 436$ mμ and $\lambda = 365$ mμ. Measurements for shorter wavelengths are not known to the author. However, a series of photomicrographs of silver bromide grains at 2500 × and 1250 × enlargements which were made by the present

author (10) at $\lambda = 450$, 365, 312, and 275 mμ show beyond doubt a rapid increase of absorption with shorter wavelengths, indicating that this increase is much greater than the energy increase of the absorbed quanta at these different wavelengths.

The highest possible value of ϵ is one. This can be approached only if the absorption coefficient of silver halide is also one. Therefore, the highest values of ϵ can occur in the far-ultraviolet region. We may, therefore, expect that the maximum sensitivity of photographic materials occurs in the far-ultraviolet region with $r = 1$.

Jones and Sandvik (7) have found that gamma and maximum gamma increase with radiation of longer wavelengths. It appears, therefore, that the approach to the maximum sensitivity of photographic material may be connected with a disappearance of gamma. This is intensified by the greater scattering of radiations in turbid media with the shorter wavelength.

SUMMARY

1. It was found empirically that in emulsion coatings producing characteristic curves representable by single-term quantic equations, there is a straight-line relation between ϵ/r and $10/i$.

2. This relation shows a definite minimum value of $\epsilon/r = 6 \times 10^{-5}$ for silver bromide and of $\epsilon/r = 4 \times 10^{-5}$ for silver bromoiodide emulsion layers containing 2.56 moles per cent of silver iodide.

3. With the data obtained for simple emulsions, the minimum size of the effective surface of the silver bromoiodide grains of a commercial emulsion were calculated and found to be of the order of 100 to 200 atoms.

4. Maximum sensitivity is most likely to be reached in the far-ultraviolet region.

Acknowledgment

The author wishes to express his thanks to Miss Helen M. Menihan for her collaboration during this investigation, and to Dr. W. West for giving suggestions concerning the determination of the minimum size of the effective surface of the grains of the commercial emulsion used.

REFERENCES

(1) R. BRUSCAGLIONI, *Ottica*, **5**, 340 (1940).
(2) L. SILBERSTEIN AND A. P. H. TRIVELLI, *J. Opt. Soc. Amer.*, **28**, 441 (1938).
(3) L. SILBERSTEIN, *Phil. Mag.*, **44**, 257 (1922).
(4) L. SILBERSTEIN AND A. P. H. TRIVELLI, *Phil. Mag.* **9**, 787, Suppl. (1930).
(5) A. P. H. TRIVELLI, JOURNAL FRANKLIN INST., **230**, 101 (1945).
(6) W. F. BERG, *Phil. Mag.* (7) **36**, 345 (1945).
(7) L. A. JONES AND O. SANDVIK, *J. Opt. Soc. Amer.*, **7**, 401 (1926).
(8) A. P. H. TRIVELLI, JOURNAL FRANKLIN INST., **241**, 85 (1946).
(9) J. EGGERT AND W. NODDACK, *Die Naturwissenschaften*, **15**, 57 (1927).
(10) A. P. H. TRIVELLI, VIII Intern. Kongress der wiss. und angew. Photographie, Dresden (1931), p. 338.

Robot Announcer Keeps Factory Abreast of the News.—A robot "announcer," on duty 24 hours a day, is keeping management employes of the Westinghouse Electric Corporation, East Pittsburgh, Pa., right up to the minute on company news. By dialing a special number on their in-plant telephones supervisory employes can listen in while a continuous tape reels off the latest developments.

Designed to keep supervisors at all levels abreast of policy matters, labor relation matters, new orders secured, production loads, backlogs, outstanding services rendered customers, quality of Westinghouse products and its effect on increasing sales, the robot announcer is saving considerable time for plant executives, T. I. Phillips, Westinghouse vice president, reported. "It now is possible to pass on a greater volume of information without any individual having to repeat the same story over and over. It's accurate too because the robot never forgets a fact or a phase."

The system works as follows: A script is prepared on the subject to be discussed, then recorded on a standard tape recorder and later transferred to a circular metallic tape which runs continuously. A system of electrical circuits amplify the message and channel it into the plant's telephone system where 30 calls can be handled at the same time—more than that get a busy signal.

The average message runs from 3 to 5 minutes in duration and new recordings are made two or three times a week. At the end of the "broadcast" an announcement is made on the time a new message may be expected. Because it takes less than half an hour to make a recording, important news can be covered quickly.

Stearns Permanent Magnetic Pulley (*Rubber Age*, Vol. 65, No. 3).—A permanent magnetic pulley which incorporates a special design of Alnico metal poles, self-energized and requiring no electrical current, was recently announced by the Stearns Magnetic Manufacturing Co., Milwaukee, Wis. The pulley is applicable for problems involving automatic removal of tramp iron from raw or processed materials, for separation of magnetic and non-magnetic products, for reclaiming secondary metals, and protection of machinery grinders, pulverizers or similar equipment. It is designed for uniform high magnetic strength over the entire face of the pulley and because no wiring or electrical connections are needed the pulley can be operated under all atmospheric and temperature conditions. More than fifty sizes are available from 12-in. diameter by 12-in. width to 30 in. by 60 in.

New Electrical Laminate (*Modern Plastics*, Vol. 26, No. 11).—A series of heavy-duty Fiber-glas reinforced Glastic electrical insulating laminates having all the requirements of high-impact class B insulating plate materials, plus flame resistance, has been announced by Laminated Plastics, Inc., Cleveland, Ohio. The new materials possess a unique combination of high rigidity, impact strength, arc and flame resistance, heat resistance, and low moisture absorption, according to the manufacturer, and are said to have already found wide use in heavy-duty apparatus by several manufacturers of electrical power equipment. Glastic plate materials are available in standard thicknesses from $\frac{1}{32}$ to $1\frac{1}{2}$ in., and in standard sheets 36 by 48 in.

STRESS-STRAIN RELATIONS IN THE PLASTIC RANGE FOR BIAXIAL STRESSES*

BY

JOSEPH MARIN[1]

1. SUMMARY

This paper gives the results of an experimental investigation on thin-walled aluminum alloy tubes subjected to combined tension and torsion. A specially designed testing machine was constructed for obtaining plastic load-strain relations to rupture for various ratios of the principal stresses ranging from 0 to −1.0. During each test, the ratios of the principal stresses were maintained essentially constant. Nominal stress-strain diagrams for the elastic range and true stress-strain diagrams for the plastic range were plotted for each test and each stress ratio.

Values of yield strength, ultimate strength, fracture strength, ductility, and plastic stress-strain relations for the various biaxial stress ratios investigated were compared with theoretical values based upon uniaxial tension results. The yield strength values were found to be in good agreement with values predicted by the Von Mises-Hencky Distortion Energy Theory. The nominal ultimate strengths, fracture strengths, ductility, and plastic stress-strain relations were approximately in agreement with the values predicted by the distortion energy theory using St. Venant's plasticity relations.

2. INTRODUCTION

The need in machine and structural design for further information on biaxial plastic stress-strain relations has led, in recent years, to many experimental investigations. The majority of these studies have dealt with plastic stress-strain relations in which both the biaxial stresses have been tensile. There have been relatively few experimental investigations on biaxial tension-compression plastic stress-strain relations (1).[2] The present paper gives the results and interpretations of combined tension-compression tests on an aluminum alloy designated as Alcoa 24S-T. Biaxial tension-compression stresses were obtained by subjecting a thin-walled tubular specimen to combined axial tension and torsion. By means of these tension-torsion tests, the influence of the biaxial stress ratio on the yield strengths, ultimate strengths, fracture strengths, ductility, and plastic stress-strain relations was determined.

3. DESCRIPTION OF MATERIAL

The material tested was a fully heat-treated aluminum alloy (Alcoa 24S-T) supplied in tubular extrusions with an internal diameter of 1 in.

* Presented at the International Congress on Applied Mechanics, London, England, September, 1948.

[1] Professor of Engineering Mechanics, Department of Engineering Mechanics, The Pennsylvania Stage College, State College, Penna.

[2] The boldface numbers in parentheses refer to the references appended to this paper.

and a wall thickness of $\frac{1}{4}$ in. The nominal chemical composition, in addition to aluminum and normal impurities, consisted of 4.4 per cent copper, 1.5 per cent magnesium, and 0.6 per cent manganese. The mechanical properties, as furnished by the manufacturer, were: tensile strength (nominal ultimate) 68,000 psi., yield strength (0.2 per cent offset) 44,000 psi., modulus of elasticity 10.6×10^6 psi., percentage elongation (in 2 in.) 14 per cent, and Poisson's ratio 0.33.

Tension tests were made on tubular specimens of the same dimensions as used for the combined stress tests (Fig. 1). The nominal and

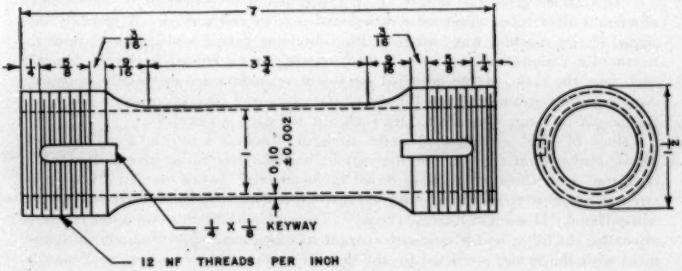

FIG. 1. Tension-torsion specimen.

true average values of the mechanical properties for three tension tests are given in Table I. In plotting the average true stress-strain diagram

TABLE I.—*Mechanical Properties of Alcoa 24S-T Tubing in Simple Tension.*

Nominal values	Yield strength (0.2% Offset)	48.1×10^3 psi.
	Ultimate strength	72.5×10^3 psi.
	Modulus of elasticity	10.7×10^6 psi.
	% Elongation (2" gage length)	11.5
True values	Fracture strength	81.0×10^3 psi.
	Ductility	0.109
	Strength coefficient k	1.14×10^5 psi.
	Strain-hardening coefficient n	0.175

for tension, as shown in Fig. 4, the true stress and true strain were defined by the equations

$$\sigma = \frac{P}{A} = \frac{P}{A_0}(1 + e_0), \tag{1}$$

$$\epsilon = \log_e (1 + e_0), \tag{2}$$

where e_0 = the nominal strain,
P = the axial load, and
A_0 = the original cross-sectional area.

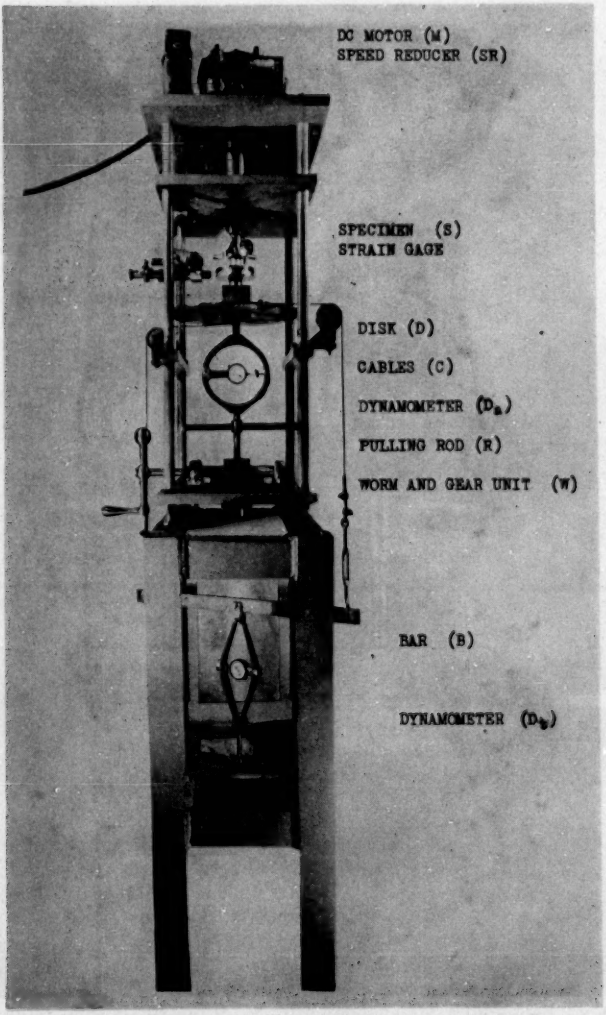

FIG. 2. Combined stress tension-torsion testing machine.

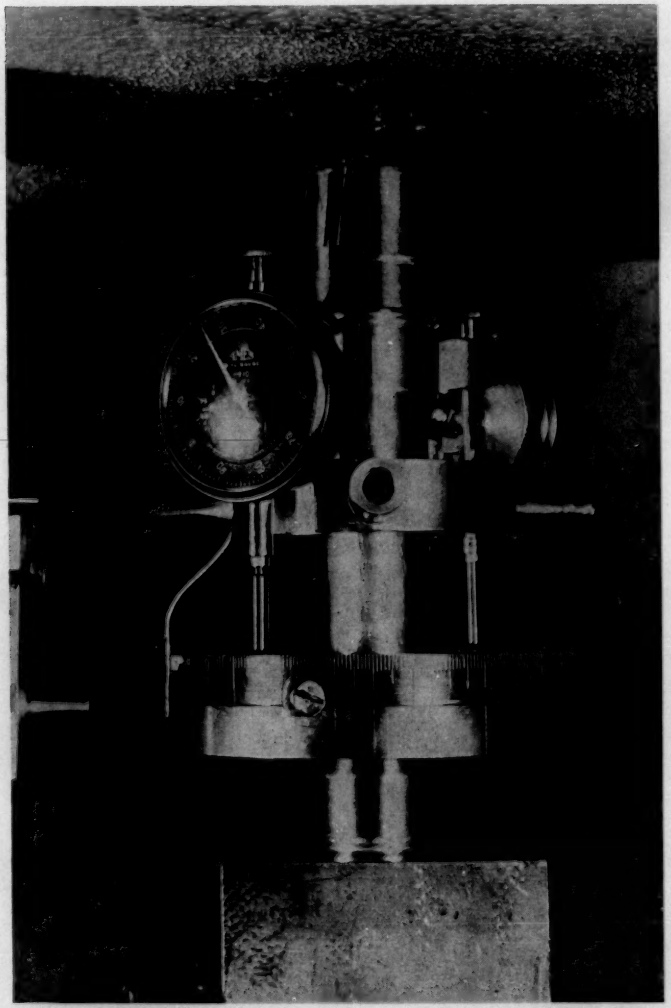

FIG. 3. Strain gage for measuring axial strain and angle of twist.

For the plastic range, many tension tests show that there is an approximate linear relation between the true stress and true strain when plotted on a log-log basis. That is, the true stress-true strain relation for ductile metals in simple tension is approximately defined by

$$\sigma = k\epsilon^n, \tag{3}$$

where k and n are experimental constants. The average values of k and n for the aluminum alloy tested are given in Table I.

4. COMBINED TENSION-TORSION TEST RESULTS

The *biaxial-stress test specimens* shown in Fig. 1 were machined from tubular sections. The dimensions were selected so that the stresses were essentially uniform throughout the wall and so that failure by buckling did not occur.

A *special testing machine* was designed for subjecting the tubular specimens to combined axial tension and torsion (Fig. 2). The axial tension load is applied to the specimen (S) by means of a worm and gear unit (W) through a pulling rod (R). The axial load is measured by a 10,000-lb. dynamometer (D_a). The twisting moment is applied by a $\frac{1}{4}$-hp. d-c. motor (M) and speed reducer (SR). Variation in speed of torque loading is provided by a rheostat of a motor-generator set. A disk (D) is attached to the lower part of the specimen to which cables are connected passing over frictionless pulleys to a bar (B). A 2000-lb. dynamometer (D_t) is attached to the bar (B) to measure the torque load.

For the *measurement of strains*, a special strain gage was designed, as shown in Fig. 3. This special gage measures both the axial strains and angles of twist in the elastic and plastic ranges. The axial strains were measured for a 2-in. gage length by two 0.0001-in. dials placed 180° apart. The angles of twist were measured for a 2-in. gage length by the twistmeter part of the gage shown in Fig. 3. Attachment of the strain gage to the specimen in the plastic range to rupture was maintained by rods which bear on the specimen at one end and are connected by preloaded springs to the strain gage at the other end. By the correct initial spring adjustment, attachment of the gage without slipping was maintained throughout the plastic range even with considerable reduction in diameter of the specimen.

The *test procedure* consisted essentially in applying torsion and tension loads of predetermined amounts corresponding to a selected value of the nominal principal stress ratio. At selected load intervals, readings of the axial strains and angles of twist were recorded for both the elastic and plastic range and up to fracture.

The test results for various principal stress ratios (σ_2/σ_1) from 0, or simple tension, to -1.0, or pure torsion, are represented by the nominal stress-strain curves in Figs. 4 and 5. In Fig. 4, the relations between the nominal axial stress σ_x' and nominal axial strain e_x are given

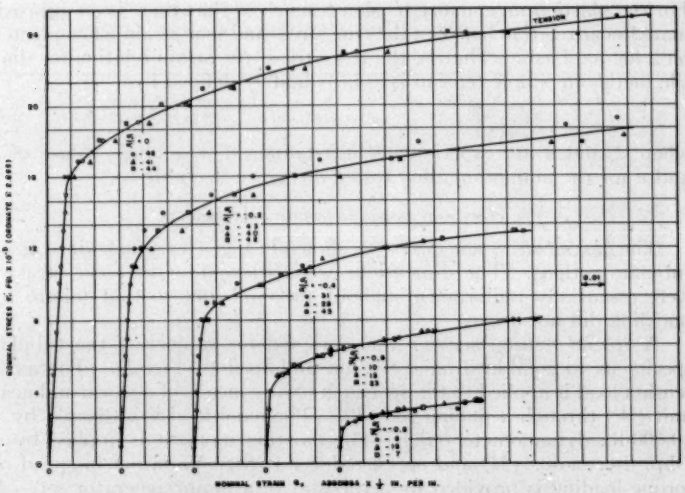

FIG. 4. Relation between normal nominal stress and strain.

NOTES: For all data in the elastic range the small circles are the average of three test results. Numerals opposite symbols are specimen numbers.

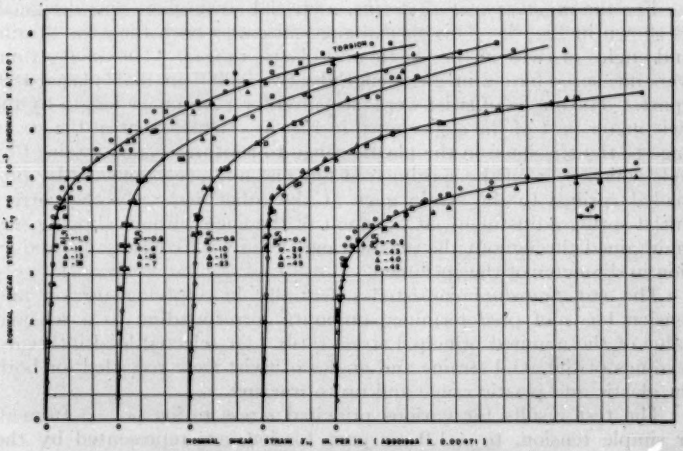

FIG. 5. Relation between nominal shear stress and nominal shear strain.

NOTES: For all data in the elastic range the small circles are an average of three test results. Numerals opposite symbols are specimen numbers.

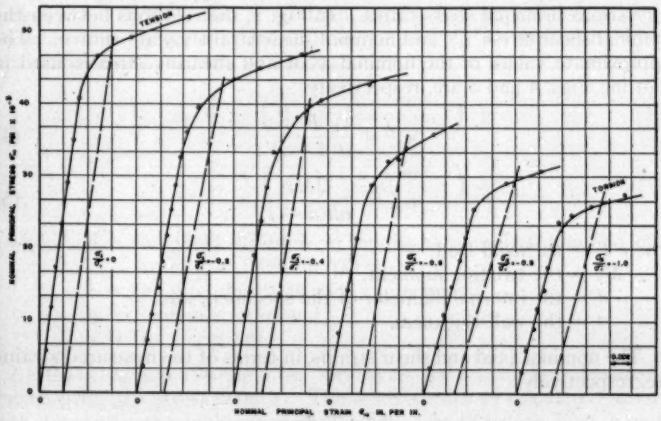

FIG. 6. Elastic stress-strain relations between principal stress σ_{1e} and principal strain e_{1e} for various biaxial stress ratios.

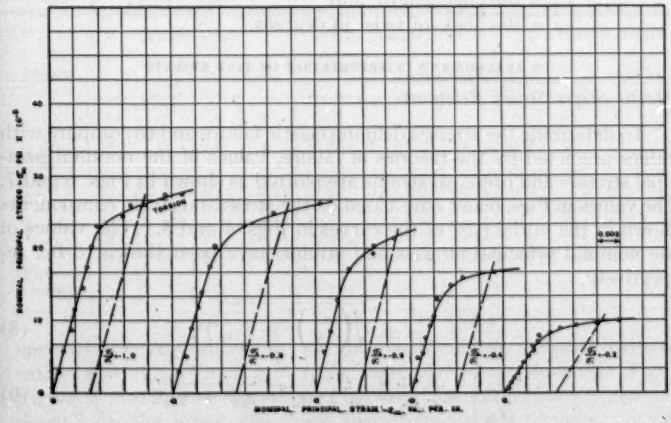

FIG. 7. Elastic stress-strain relations between principal stress $-\sigma_{2e}$ and principal strain $-e_{2e}$ for various biaxial stress ratios.

for various principal stress ratios. In Fig. 5, the relations between the nominal shear stress τ_{xy}' and nominal shear strain γ_{xy} are shown. The approximate values of the nominal axial and shearing stresses used in plotting Figs. 4 and 5 are, respectively,

$$\sigma_x' = \frac{P}{\pi t(d + t)}, \tag{4}$$

$$\tau_{xy}' = \frac{2M_t}{\pi dt(d + t)}, \tag{5}$$

where P = the axial load,
M_t = the twisting moment,
d = the internal diameter of the specimen, and
t = the wall thickness.

The nominal axial and shear strains, in terms of the measured strains are, respectively,

$$e_x = \frac{\delta_{1x} + \delta_{2x}}{2L_0}, \tag{6}$$

$$\gamma_{xy} = \frac{\pi}{720}(d + 2t)\rho, \tag{7}$$

where δ_{1x}, δ_{2x} = the measured axial strains on two sides of the specimen,
L_0 = the gage length, and
ρ = the angle of twist in degrees.

5. ANALYSIS AND INTERPRETATION OF TEST RESULTS

Elastic Stress-Strain Relations

To determine the stresses defining elastic failure and to compare with values predicted by the theories of failure, values of the nominal principal stresses and principal strains are plotted as shown in Figs. 6 and 7. The values in Figs. 6 and 7 are based on the stress and strain components shown in the initial part of the curves in Figs. 4 and 5. The values of the nominal principal stresses and strains have been shown to be, respectively,

$$\left.\begin{matrix}\sigma_{1e}\\ \sigma_{2e}\end{matrix}\right\} = \frac{\sigma_x'}{2} \pm \sqrt{\left(\frac{\sigma_x'}{2}\right)^2 + (\tau_{xy}')^2}, \tag{8}$$

$$\left.\begin{matrix}e_{1e}\\ e_{2e}\end{matrix}\right\} = \frac{e_x + e_y}{2} \pm \tfrac{1}{2}\sqrt{(e_x - e_y)^2 + \gamma_{xy}^2}. \tag{9}$$

To define elastic failure or yielding, the yield strength in simple tension will be based on an offset strain of 0.002 in. per in., as shown in Fig. 6. For combined stresses an equivalent offset strain value (2),

equivalent to the value of 0.002 in. per in. for simple tension, will be used. The equivalent offset strain e_{01} and e_{02} corresponding to the principal strains e_{1e} and e_{2e} are (2)

$$e_{01} = \frac{\sigma_y'}{E}\left(1 - \frac{1 - m\alpha}{\sqrt{1 - \alpha + \alpha^2}}\right) + e_t, \qquad (10a)$$

$$e_{02} = \frac{\sigma_y'}{E}\left(1 - \frac{\alpha - m}{\sqrt{1 - \alpha + \alpha^2}}\right) + e_t, \qquad (10b)$$

where σ_y' = the yield strength in simple tension based on an offset strain $e_t = 0.002$ in. per in.,
E = the modulus of elasticity in tension,
m = Poisson's ratio, and
α = the stress ratio.

By Eqs. 10*a* and 10*b* the offset strains e_{01} and e_{02} can be calculated for each principal stress ratio α. The offset strains so calculated are used to determine the yield stresses σ_{2y} and σ_{1y} as shown in Figs. 6 and 7. The values of these yield stresses, representing the average of three tests, are given in Table II. To compare the biaxial yield strength values with values predicted by the theories of failure, the principal stress ratios $x = \sigma_{1y}/\sigma_y'$ and $y = \sigma_{2y}/\sigma_y'$ are plotted as shown in Fig. 8. Figure 8 also shows the relation between the stress ratios x and y, as defined by the shear, distortion energy, and stress theories. A comparison between the test results and the theories of failure shows that the test results are in closest agreement with the distortion energy theory.

TABLE II.—*Biaxial Yield, Ultimate and Fracture Strengths for Various Biaxial Stress Ratios.*

NOTE: Each value recorded is based on an average of three tests. Stress values given in table are in psi. $\times 10^{-3}$. Stress ratios $x = \sigma_1/\sigma$ and $y = \sigma_2/\sigma$.

$\alpha = \sigma_2/\sigma_1$	Yield Strength				Nominal Ultimate Strength				True Fracture Strength			
			Stress Ratios				Stress Ratios				Stress Ratios	
	σ_{1y}	σ_{2y}	x	y	σ_{1u}	σ_{2u}	x	y	σ_{1r}	σ_{2r}	x	y
0 (Simple tension)	48.1	0	1.0	0	72.5	0	1.0	0	81.0	0	1.0	0
−0.2	42.4	− 9.9	0.88	−0.21	67.0	−13.4	0.93	−0.18	67.9	−14.0	0.84	−0.17
−0.4	39.4	−16.8	0.82	−0.35	59.8	−23.5	0.83	−0.32	63.5	−25.4	0.79	−0.31
−0.6	33.5	−21.7	0.70	−0.45	55.8	−33.4	0.77	−0.46	59.4	−35.8	0.73	−0.44
−0.8	29.6	−24.3	0.62	−0.51	50.6	−40.4	0.70	−0.56	51.0	−40.9	0.63	−0.51
−1.0 (Pure torsion)	26.3	−26.3	0.55	−0.55	44.8	−44.8	0.62	−0.62	44.8	−44.8	0.55	−0.55

Plastic Stress-Strain Relations

To determine the plastic stress-strain relations, the changes in the dimensions of the specimens must be considered. In the plastic range these changes in dimensions are appreciable and the stresses and strains can no longer be based on the original dimensions and gage length.

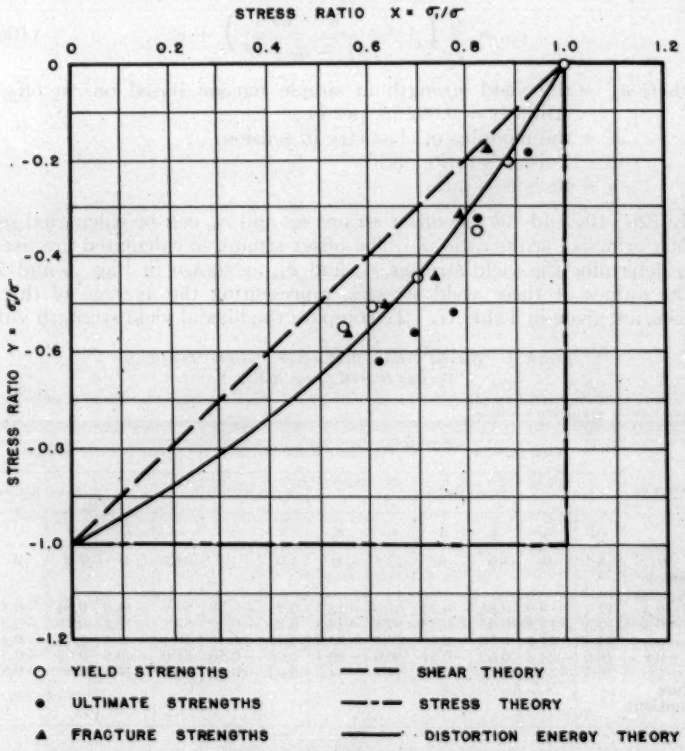

FIG. 8. Comparison of actual and theoretical strengths for various ratios of the principal stresses from 0 to −1.0.

True stresses and strains based on change in dimensions must now be used in place of the nominal values given by Eqs. 8 and 9.

The true stress components σ_x and τ_{xy} can still be defined by Eqs. 4 and 5 provided the original values of d and t in these equations are replaced by their true values.

To determine the true value of wall thickness (t_p) we can write, using Eq. 2, the true strain in the direction of the wall thickness as

$$\epsilon_z = \log_e (1 + e_x) = \log_e \frac{t_p}{t}. \tag{a}$$

If the volume is assumed to remain constant in the plastic range, $\epsilon_x + \epsilon_y + \epsilon_z = 0$. Since $\sigma_y = 0$ and $\sigma_2 = 0$, then $\epsilon_y = -\epsilon_z$ or

$$\epsilon_z = -\frac{\epsilon_x}{2} = -\tfrac{1}{2} \log_e (1 + e_x). \tag{b}$$

From Eqs. a and b the wall thickness t_p in terms of the original wall thickness is

$$t_p = t/(1 + e_x)^{\frac{1}{2}}. \tag{c}$$

The *true value of the diameter* (d_p) is given by

$$\epsilon_z = \log_e d_p/d. \tag{d}$$

From Eqs. b and d,

$$d_p = d/(1 + e_x)^{\frac{1}{2}}. \tag{e}$$

Replacing the values of d and t in Eqs. 4 and 5 with d_p and t_p from Eqs. c and e, the true stress components σ_x and τ_{xy} are

$$\sigma_x = \frac{P}{\pi t(d + t)} (1 + e_x) = \sigma_x'(1 + e_x), \tag{11}$$

$$\tau_{xy} = \frac{2M_t}{\pi dt(d + t)} (1 + e_x)^{\frac{1}{2}} = \tau_{xy}'(1 + e_x)^{\frac{1}{2}}. \tag{12}$$

The *true principal stresses* corresponding to the true stress components σ_x and τ_{xy} are

$$\left.\begin{matrix}\sigma_1 \\ \sigma_2\end{matrix}\right\} = \frac{\sigma_x}{2} \pm \sqrt{\left(\frac{\sigma_x}{2}\right)^2 + \tau_{xy}^2}. \tag{13}$$

The directions of the planes of principal stresses are defined by the values

$$\left.\begin{aligned}\theta_1 &= \frac{1}{2}\left[\tan^{-1}\left(\frac{-2\tau_{xy}}{\sigma_x}\right)\right] \\ \theta_2 &= \frac{\pi}{2} + \theta_1.\end{aligned}\right\} \tag{14}$$

The values of θ_1 and θ_2 determine the direction of the planes perpendicular, respectively, to the stresses σ_1 and σ_2.

The *true principal strains* will be defined as the strains in the direction of the true principal stresses. The values of the principal strains in terms of the nominal strains e_x and γ_{xy} are defined by Eqs. 24 and 22 given in Appendix 1. In calculating the true principal stresses and strains, values of the nominal stress and strain components are selected

from the average curves shown in Figs. 4 and 5. The values of the true principal stresses and strains computed in this manner are plotted in Figs. 9 and 10. The principal stress ratios shown on the curves of Figs. 8 and 9 represent approximate values, since these ratios are based

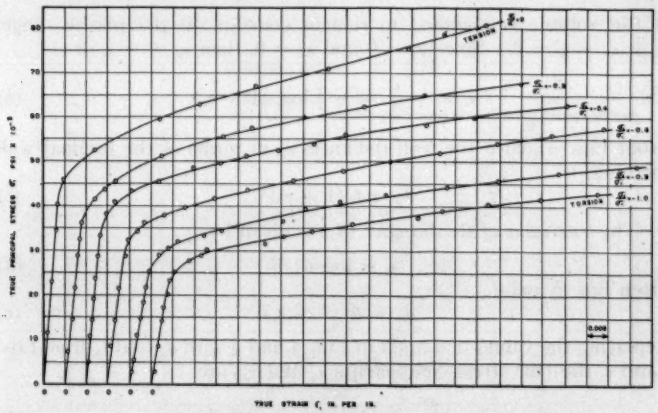

FIG. 9. Relation between true principal stress σ_1 and true strain ϵ_1 for various biaxial stress ratios.

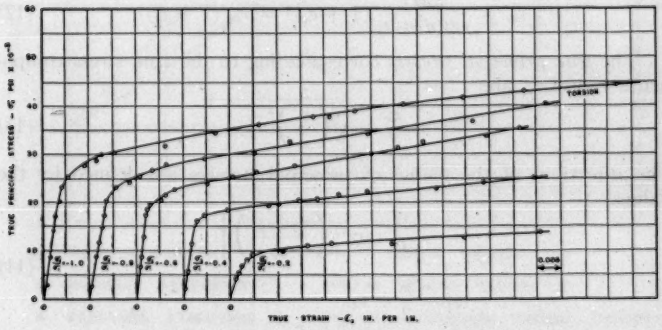

FIG. 10. Relation between true principal stress $-\sigma_2$ and true strain $-\epsilon_2$ for various biaxial stress ratios.

on nominal stress calculations. With the test results in the form of true principal stresses and strains, it is now possible to compare the test results with theoretical values.

Several theories have been proposed to define the true plastic combined stress-strain relations in terms of the stress-strain relation for

simple tension. These theories are of two types, either flow theories or deformation theories, as discussed in several papers including those by Ilyushin (3), Handelman, Lin and Prager (4), and Prager (5, 6). In the loading condition considered in this investigation, and for tests in which the ratio of the principal stresses remains essentially constant, the flow and deformation theories agree. Most of the recent experimental investigations on plastic combined stress-strain relations have used the deformation type theory for interpretation of the test results.

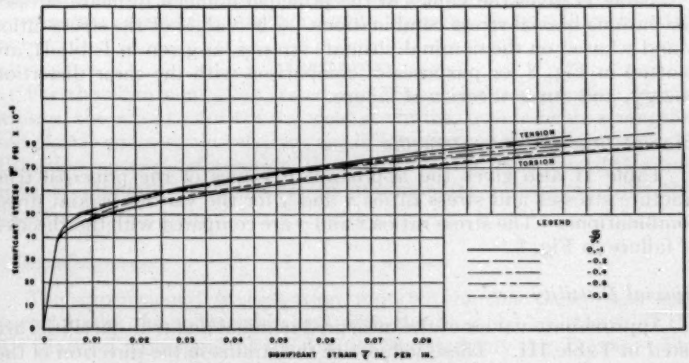

FIG. 11. Comparison of significant stress-significant strain relations for various biaxial stress ratios.

The following interpretation of the plastic stress-strain relations will utilize the deformation type theory based on distortion energy since this theory was found to be in better agreement with the test results than the shear theory (9). The theory used defines a stress and strain, called the significant stress and strain (7, 8, 9).[3] For biaxial stresses the values of the significant stress and strain have been shown to be (10)

$$\bar{\sigma} = \sqrt{\sigma_1^2 - \sigma_1\sigma_2 + \sigma_2^2}, \tag{15}$$

$$\bar{\epsilon} = \sqrt{\frac{4}{3}(\epsilon_1^2 + \epsilon_1\epsilon_2 + \epsilon_2^2)}. \tag{16}$$

Using the values of the principal stresses (σ_1, σ_2) and strains (ϵ_1, ϵ_2) shown in Figs. 9 and 10 in Eqs. 15 and 16, the significant stresses and strains can be determined and the values plotted as shown in Fig. 11. For simple tension, by Eqs. 15 and 16, $\bar{\sigma} = \sigma_t$ and $\bar{\epsilon} = \epsilon_t$. That is, by this theory, the significant stress-strain relation for simple tension should coincide with the true stress-strain diagram for simple tension.

[3] The significant stress and strain are equivalent to the effective stress-strain and octahedral shear stress-strain as defined in various reports.

Figure 11 shows that there is an approximate agreement between the significant stress-strain relations for the various biaxial stress ratios and the true stress-strain relation for simple tension. That is, in terms of the stress, the maximum difference between the significant stress values as defined by the distortion energy theory and by test results is about 6 per cent.

Biaxial Nominal Ultimate Strengths

Table II gives the values of the principal nominal ultimate stresses for various biaxial stress combinations. The values of the stress ratios x and y based on the nominal ultimate stresses, as given in Table II, are plotted in Fig. 8 for purposes of comparison with the shear distortion energy, and stress theories of failure.

Biaxial True Fracture Strengths

Table II also gives the approximate values of the principal true fracture stresses and stress ratios x and y for the various biaxial stress combinations. The stress ratios x and y are compared with the theories of failure in Fig. 8.

Biaxial Ductility

Approximate values of the measured nominal and true ductilities are listed in Table III. These values are the strains in the direction of the

TABLE III.—*Nominal and True Ductilty Values for Various Ratios of Biaxial Stresses.*

Biaxial Stress Ratio	Measured Nominal Ductility* in. per in.	True Ductility (ϵ_1 Values)		
		Measured in. per in.	Theoretical in. per in.	% Diff.
0 (Long. tension)	0.088	0.084	0.096	+14
−0.2	0.111	0.105	0.100	− 5
−0.4	0.118	0.112	0.119	+ 6
−0.6	0.134	0.126	0.149	+18
−0.8	0.149	0.139	0.117	−16
−1.0 (Pure torsion)	0.148	0.122	0.096	−21

* Principal strain value e_1 prior to fracture.

maximum principal stresses and are based on the measured strains just prior to fracture. The theoretical value of the true ductility based on the distortion energy theory has been shown to be (10)

$$\epsilon_{1r} = \left(\frac{\sigma_r}{k}\right)^{1/n} (\alpha^2 - \alpha + 1)^{(1-n)/2n} \left(1 - \frac{\alpha}{2}\right), \qquad (17)$$

where $\alpha = \sigma_2/\sigma_1$ = the principal stress ratio,
σ_r = true fracture strength in simple tension, and
k and n = material constants for simple tension.

With average values of k and n as given in Table I and the average value of σ_r based on three tests, the theoretical values of the true ductilities ϵ_{1r} were calculated by Eq. 17 for various values of the principal stress ratio α. These values are shown in Table III and are compared with the actual true ductilities. In view of the inaccuracies and difficulties involved in obtaining the values of both the theoretical and experimental ductilities, the agreement between these values is satisfactory.

CONCLUSIONS

For the aluminum alloy tested and for tension-compression biaxial stresses, the actual values of the yield strengths, true fracture strengths, and plastic stress-strain relations are in satisfactory agreement with the distortion energy deformation theory, while the true ductilities and nominal ultimate strengths are in approximate agreement with this theory.

Acknowledgments

The experimental investigation reported in this paper was conducted under the sponsorship and with the financial assistance of the Air Materiel Command of the United States Army Air Forces. The tests were conducted in the Combined Stress Laboratory, Department of Engineering Mechanics, The Pennsylvania State College. The writer gratefully acknowledges the help of Dr. J. A. Sauer in the preparation of this paper and the assistance of Messrs. J. H. Faupel and V. L. Dutton, Research Assistants, who obtained the test data and plotted the results.

REFERENCES

(1) W. LODE, "Der Einfluss der Mittleren Hauptspannung suf das Fliessen der Metalle," *Forsch.-Arb. Geb. Ing.-Wes.*, VDI-Verlag B.M.B.H. (Berlin), Heft 303 (1928).

B. I. TAYLOR, AND H. QUINNEY, "The Plastic Distortion of Metals," *Phil. Trans. Royal Soc.* (London), Ser. A, Vol. 230, Nov. 13, 1931, pp. 323–362.

J. MARIN, AND R. L. STANLEY, "Failure of Aluminum Subjected to Combined Stresses," Supplement, *J. Am. Welding Soc.*, Feb., 1940.

J. SEIGLE, AND F. CRETIN, "The Elastic Limit and Resistance of Annealed Mild Steel in the Case of Combined Tension and Torsion" (French), *Revue de Metallurgie Memoirs*, Vol. 22, June, 1925.

E. A. DAVIS, "Combined Tension-Torsion Tests on a 0.35% Carbon Steel," *Trans. A.S.M.E.*, Vol. 62, No. 7, Oct. 1940.

(2) J. MARIN, "Mechanical Properties of Materials and Design," McGraw-Hill Book Co., 1942, Chapter 1.

(3) A. A. ILYUSHIN, "Relations Between the Theory of St. Venant-Levy-Mises and the Theory of Small Elastic-Plastic Deformations." Translation by Appl. Math. Group, Brown Univ., 1945 for the David W. Taylor Model Basin, U. S. Navy. (From *Prikl. Mat. i Mekh.*, Moscow, Vol. 9, 1945, pp. 207–218.)

(4) G. H. HANDELMAN, C. C. LIN, AND W. PRAGER, "On the Mechanical Behavior of Metals in the Strain-Hardening Range," *Quarterly Appl. Math.*, Vol. IV, No. 4, Jan. 1947, pp. 397–407.
(5) W. PRAGER, "Strain Hardening Under Combined Stresses," *J. Appl. Phys.*, Vol. 16, No. 12, Dec., 1945, pp. 837–840.
(6) W. PRAGER, "On the Interpretation of Combined Torsion and Tension Tests of Thin-Wall Tubes," *Tech. Note 1501*, N.A.C.A., Washington, D. C., Jan., 1948.
(7) M. GENSAMER, W. T. LANKFORD, J. RANSOM, J. VAJDA, AND T. A. PRATER, "Plastic Flow of Aluminum Aircraft Sheets Under Combined Loads," Final Report, NDRC Project NRC 51, 1945.
(8) J. V. JELINEK, A. J. LATTER, E. G. THOMSEN, AND J. E. DORN, "Plastic Flow in Metals," OPRD Research Project NRC-548, May 1945. 243 pages.
(9) W. R. OSGOOD, "Combined Stress Tests on 24S-T Aluminum Alloy Tubes," *J. Appl. Mech.*, A.S.M.E., Sept., 1947.
(10) J. MARIN, J. H. FAUPEL, V. L. DUTTON, AND M. W. BROSSMAN, "Biaxial Plastic Stress-Strain Relations for Alcoa 24S-T," *N.A.C.A. Technical Note No. 1536*, 1948.

APPENDIX I

Determination of True Principal Strains

The plastic deformation of the element in Fig. 12(*a*) is shown in Fig. 12(*b*). The torsional stress results in motion of B toward B_1 and the axial stress in movement of B to B_3. If the element has a unit length $\overline{AC}$, then the shear strain = $\tan \overline{BGB_1} = \tan \gamma_{xy}$. Also, $\overline{B_3J} = e_x$ = the nominal axial strain and $B_1J = (e_y)(\overline{AG})$ where e_y = the nominal lateral strain. In this case, $\sigma_y = 0$, and for constancy of volume, $e_y = \frac{1}{2}e_x$. Referring again to Fig. 12(*b*), a line $\overline{AB}$ before the stresses are applied moves to $\overline{AB_3}$ so that the nominal strain for $\overline{AB}$ will be defined by

$$e' = \frac{\overline{EB_3}}{\overline{AB}}. \tag{a}$$

It should be noted that the definition of the strain given by Eq. *a* is an arbitrary one since the reference line $\overline{AB}$ changes in direction as the stresses are applied. However, it is expected that the errors produced by the foregoing assumption are small. In any case, the procedure used may be considered as approximate.

By a consideration of triangles ABE and BEB_3,

$$\overline{EB_3} = \overline{AB}[\cos(\beta - \alpha) + \sin(\beta - \alpha)\cot\gamma - 1]. \tag{b}$$

Placing the value of $\overline{EB_3}$ from Eq. *b* in Eq. *a*,

$$e' = \cos(\beta - \alpha) + \sin(\beta - \alpha)\cot\gamma - 1. \tag{c}$$

Applying the Sine Law to triangle ABB_3,

$$\sin\gamma = \frac{\overline{AB}}{\overline{BB_3}}\sin(\beta - \alpha). \tag{d}$$

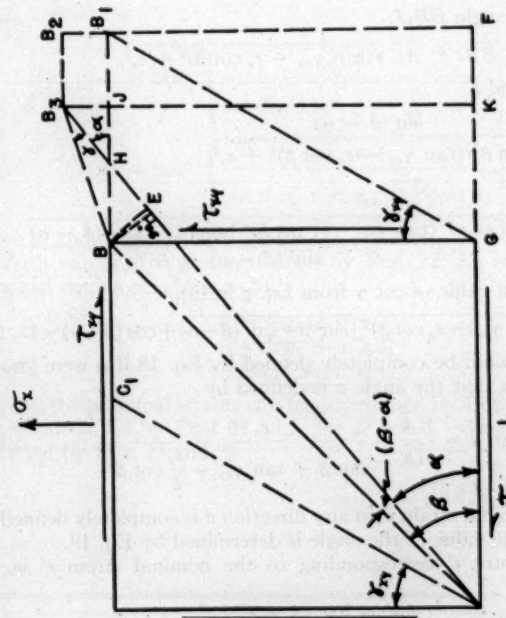

FIG. 12(b). Deformation of element subjected to axial stress and shear stress.

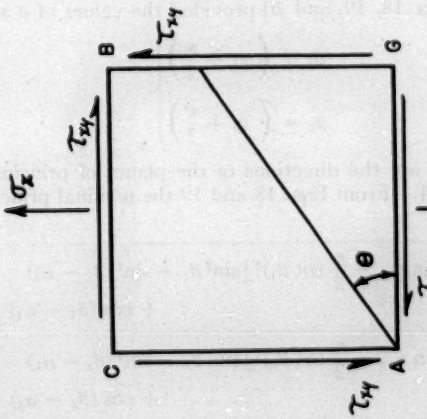

FIG. 12(a). Stress components.

Considering triangle BB_3J,

$$\overline{BB_3} = \overline{AC}\sqrt{(\tan \gamma_{xy} - e_y \cot \beta)^2 + e_x^2}. \tag{e}$$

From Eqs. d and e,

$$\sin \gamma = \frac{\sin (\beta - \alpha)}{\sin \beta \sqrt{(\tan \gamma_{xy} - e_y \cot \beta)^2 + e_x^2}} \tag{f}$$

or

$$\cot \gamma = \sqrt{\frac{[e_x^2 - (\tan \gamma_{xy} - e_y \cot \beta)^2] \sin^2 \beta - \sin^2 (\beta - \alpha)}{\sin^2 (\beta - \alpha)}}. \tag{g}$$

Substituting the value of cot γ from Eq. g in Eq. c,

$$e' = \sqrt{[e_x^2 + (\tan \gamma_{xy}) - e_y \cot \beta)^2] \sin^2 \beta - \sin^2 (\beta - \alpha)} + \cos (\beta - \alpha) - 1. \tag{18}$$

The strain e_β would be completely defined by Eq. 18 if α were known. It can be shown that the angle α is defined by

$$\tan \alpha = \frac{\overline{B_3k}}{\overline{Ak}} = \frac{e_x + 1}{\cot \beta + \tan \gamma_{xy} - \frac{e_x}{2} \cot \beta}. \tag{19}$$

That is, the nominal strain e' in any direction β is completely defined by Eq. 18 where the value of the angle is determined by Eq. 19.

The *true strain* ϵ' corresponding to the nominal strain e' is, by Eq. 2,

$$\epsilon' = \log_e (1 + e'). \tag{20}$$

The *true principal strains* will be defined as those strains in the direction of the principal stresses. The values of these strains can be determined by Eqs. 18, 19, and 20 provided the values of β are taken as

$$\left.\begin{aligned} \beta_1 &= \left(\theta_1 + \frac{\pi}{2}\right) \\ \beta_2 &= \left(\theta_2 + \frac{\pi}{2}\right) \end{aligned}\right\}, \tag{21}$$

where θ_1 and θ_2 are the directions of the planes of principal stress as given by Eqs. 14. From Eqs. 18 and 19 the nominal principal strains are

$$\left.\begin{aligned} e_1 &= \sqrt{[e_x^2 + (\tan \gamma_{xy} - \frac{e_x}{2} \cot \beta_1)^2] \sin^2 \beta_1 - \sin^2 (\beta_1 - \alpha_1)} \\ &\qquad + \cos (\beta_1 - \alpha_1) - 1, \\ e_2 &= \sqrt{[e_x^2 + (\tan \gamma_{xy} - \frac{e_x}{2} \cot \beta_2)^2] \sin^2 \beta_2 - \sin^2 (\beta_2 - \alpha_2)} \\ &\qquad + \cos (\beta_2 - \alpha_2) - 1, \end{aligned}\right\} \tag{22}$$

where

$$\left.\begin{aligned}\alpha_1 &= \tan^{-1}\left[\frac{e_x + 1}{\cot \beta_1 + \tan \gamma_{xy} - \frac{e_x}{2}\cot \beta_1}\right] \\ \alpha_2 &= \tan^{-1}\left[\frac{e_x + 1}{\cot \beta_2 + \tan \gamma_{xy} - \frac{e_x}{2}\cot \beta_2}\right]\end{aligned}\right\}, \tag{23}$$

where β_1 and β_2 are defined by Eqs. 21.

With values of e_1 and e_2 defined by Eqs. 22, 23, and 21, the true principal strains are, by Eq. 20,

$$\left.\begin{aligned}\epsilon_1 &= \log_e (1 + e_1) \\ \epsilon_2 &= \log_e (1 + e_2) \\ \epsilon_3 &= -(\epsilon_1 + \epsilon_2)\end{aligned}\right\}. \tag{24}$$

That is, the principal strains can be determined by Eqs. 24 when e_1 and e_2 are calculated by Eqs. 22 with the α and β values in Eqs. 22 determined by Eqs. 23 and 21.

Portable Dark Room.—The Camera Specialty Company has been appointed exclusive distributors for the new Bendick Portable Dark Room. This new unit now makes it possible for amateur and professional photographers to process their film, load holders, make prints in brilliant sunlight or anywhere, any time of day with absolute safety.

The Bendick Portable Dark Room replaces the old changing bag. Now the photographer can get right into this portable dark room, switch on the light and prepare his accessories for processing. The light can be snapped off in a hurry and complete finished pictures can be made without waiting to take them to the studio to complete the job. Summertime is no handicap as there is a removable cooling system if needed; uses ice cubes or dry ice in a non-rust cylinder.

The Bendick Portable Dark Room folds up smaller than a rain coat. It weighs 3½ lb. and is only 12 in. long. It is absolutely light tight and is made of high grade porous material.

Westinghouse Precipitron Aids Technicolor in Keeping Film Free of Defects.—Although cleanliness of air is of great importance in many industrial processes, few plants have as great a need for clean-as-humanly-possible air as the celebrated Technicolor plant in Hollywood. In the processing of *motion picture film in color*, any microscopic speck on the postage-stamp-sized frame becomes huge when the image is projected on a theater screen, at a magnification varying from 200 to 300 times.

Furthermore, the film *consists of a gelatin coating on a plastic base*, and *it therefore tends* to hold an electrical charge. This characteristic, in turn, *causes the film to attract* and hold any particle—however microscopic—of dust or foreign matter in the air *around it*.

As a result, the Technicolor Motion Picture Corporation must necessarily keep its premises—particularly the areas where film is handled and processed—spotlessly clean. This task has recently been considerably facilitated in these areas by an extensive installation of Westinghouse Precipitron apparatus, which is in various air intakes of the building's air-conditioning system. Every minute, 133,000 cubic feet of air pass through the Precipitron apparatus. Sizes of the Precipitron vary from 24,000 CFM capacity down to 4,800 CFM.

Although the Precipitron installation is so new that no accurate figures on its performance are available as yet, "it has already had a very noticeable effect on our building maintenance, by making it easier to keep our film-processing areas clean," according to Dr. Herbert T. Kalmus, President of the Technicolor Motion Picture Corporation.

V.2
194

PREPARATION OF VANADIUM PENTOXIDE SOLS BY ION EXCHANGE

BY

JAMES A. DEVLIN,[1] WALLACE M. McNABB[1] AND FRED HAZEL[1]

The most widely used method for the preparation of vanadium pentoxide sols involves addition of an acid to ammonium vanadate, washing the precipitated oxide until it begins to peptize and then suspending in water until dispersion is complete (1).[2] The sols contain a variable amount of molecular vanadium pentoxide, depending on their age (5). The molecular fraction passes through dialyzing membranes and, since it is in equilibrium with the colloidal particles, purification of the system by dialysis is accompanied by continuous loss of vanadium. The preparation of a sol of low electrolyte content has been reported by Prandtl and Hess (4). The method consisted of hydrolyzing the tertiary butyl ester of orthovanadic acid followed by distillation of the alcohol.

This report describes the preparation of a relatively pure vanadic acid system from ammonium vanadate by the method of ion exchange. A batch procedure has been employed because of the low solubility of the starting material.

EXPERIMENTAL

The exchange resins, Amberlite IR-100H and Dowex-50, were conditioned by three sodium-hydrogen cycles and used in the hydrogen form.

Sol I.

A weighed amount of C.P. ammonium vanadate, 1.0479 g., was mixed with 10 ml. of water and 15.0 g. of air-dried Amberlite IR-100H. The paste was stirred until it acquired a deep red color. This occurred in about five minutes. One hundred ninety ml. of water was added with rapid stirring. The system had the deep color characteristic of V_2O_5 sols. It was filtered and analyzed for ammonia (6) and vanadium (3).

Sol II.

A weighed amount of ammonium vanadate, 21.1688 g., was mixed

[1] Department of Chemistry and Chemical Engineering, University of Pennsylvania, Philadelphia, Penna.

[2] The boldface numbers in parentheses refer to the references appended to this paper.

with one liter of water and 300 ml. of wet Dowex-50. The system was stirred one hour, filtered and the sol analyzed.

RESULTS

Analyses of the Sols

TABLE I.

Weights on a Liter Basis	Sol I	Sol II
Wt. of NH_4VO_3 taken/liter	4.1916 g.	21.1688 g.
Wt. of V taken	1.8255	9.2189
Amount resin used	60.0	300 ml. (ca. 138 g.)
Wt. V in sol, total	1.1780	5.3060
Wt. V as V_2O_5 in sol	1.1289	5.0134
Wt. V as NH_4VO_3 in sol	0.0491	0.2926
Per cent conversion to V_2O_5	61.84	54.38
pH of sol	2.8	2.4

Clouding Values

Clouding values (7), indicating the concentrations of electrolytes required to coagulate the colloidal system, were determined by adding 2.0 ml. of sol to 3.0 ml. of electrolyte and observing after 24 hours. The data, recorded in Table II, reveal that the particles were negatively charged.

TABLE II.

Electrolyte	Clouding Value, m.eq. per liter	Remarks
NH_4Cl	8.0	Weak gel
NH_4VO_3	13.6	Weak gel
$BaCl_2 \cdot 2H_2O$	0.64	
$LaCl_3 \cdot 7H_2O$	0.60	

DISCUSSION

The reaction occurring in the preparation of the sol may be expressed as follows:

$$\underset{\text{solid}}{NH_4VO_3} \downarrow \quad \underset{\text{dissolved}}{NH_4^+ + VO_3^-} + R \cdot H \rightleftharpoons R \cdot NH_4 + HVO_3 \quad \Updownarrow \quad \underset{\text{colloidal}}{V_2O_5 \cdot xH_2O}$$

The formation of a colloidal product shifts the reaction to the right.

It was found that an excess of resin was required for the production of a stable sol. Calculated amounts of reactants yielded a precipitate because of the coagulating action of ammonium vanadate present in the equilibrium system. Results indicate that excess resin, however, contributed to the low yield of V_2O_5 in the sol. It was shown by quali-

tative tests that the resin adsorbed pentavalent vanadium. A mechanism similar to the following may be suggested for the adsorption.

$$V_2O_5 + 2H^+ + 3H_2O \rightleftharpoons 2V(OH)_4^+$$
$$V(OH)_4^+ + R\cdot H \rightleftharpoons R\cdot V(OH)_4 + H^+.$$

The lower yield of V_2O_5 in Sol II may be attributed to the above reactions and the use of the resin with the greater exchange capacity, Dowex-50, in the preparation of this system.

The Amberlite resin caused partial reduction of vanadate to vanadyl ion, which then competed with the ammonium ion for exchange on the resin.

$$VO^{++} + 2R\cdot H \rightleftharpoons R\cdot VO + 2H^+$$

On regenerating the resin with hydrochloric acid, the reaction was shifted to the left and the solution acquired the blue color of the vanadyl ion. The reducing property of this resin has been reported previously (2). Dowex-50 proved to be more stable in the presence of vanadate. However, on contact with the solution for several days, this resin showed some reducing action.

The chemical properties of vanadic acid prepared by ion exchange are being investigated.

REFERENCES

(1) W. BILTZ, *Ber.*, Vol. 37, p. 1098 (1904).
(2) G. E. BOYD, J. SCHUBERT AND A. W. ADAMSON, *J. Am. Chem. Soc.*, Vol. 69, p. 2818 (1947).
(3) W. F. HILLEBRAND AND G. E. F. LUNDELL, "Applied Inorganic Analysis," p. 359. New York, John Wiley & Sons, Inc., 1929.
(4) W. PRANDTL AND L. HESS, *Z. anorg. Chem.*, Vol. 82, p. 116 (1913).
(5) W. REINDERS AND G. VAN DER LEE, *Rec. trav. chim.*, Vol. 47, p. 193 (1928).
(6) E. C. WAGNER, *Ind. Eng. Chem., Anal. Ed.*, Vol. 12, p. 771 (1940).
(7) H. B. WEISER, "Inorganic Colloid Chemistry," Vol. II, p. 295. New York, John Wiley & Sons, Inc., 1935.

NOTES FROM THE NATIONAL BUREAU OF STANDARDS*

PANEL-TYPE ACCELEROMETER FOR AIRCRAFT

A novel type of accelerometer[1] which gives both an instantaneous indication and record of the acceleration of an airplane in flight has been developed by A. S. Iberall of the National Bureau of Standards for the U. S. Air Force. Outstanding features of the device are compactness, which permits mounting on an instrument panel, and the use of spark recording to obtain a readily available record on a paper chart. The details of the design are such that small panel-type recorders of other physical quantities—temperature, pressure, or voltage, for example—can be similarly constructed to occupy a space not much larger than an ordinary indicating instrument.

The immediate application of the new accelerometer is in the training of aviators for combat flying, where sharp turns must be made at high speeds. Practice in making such turns can be more effectively obtained if the instrument panel of the plane is provided with an accelerometer that gives an instantaneous visual indication of acceleration while the maneuver is being executed. At the same time, it is desirable to have a record of acceleration for quick reference after a flight has been completed. However, the accelerometers that have been available are either too large for instrument-panel mounting or, if small enough for panel use, do not provide an automatic record of acceleration. Moreover, as most recording accelerometers require photographic equipment, interpretation of the trace must usually wait until the film has been developed. The Air Force therefore requested the National Bureau of Standards to undertake the development of a small, compact indicating and recording accelerometer that would meet the requirements of flight training use.

A sliding bob mounted on a shaft and restrained by a helical spring serves as the acceleration-sensitive element of the device. Acceleration of the aircraft along the axis of the shaft displaces the bob by an amount proportional to the acceleration, at the same time compressing the spring. The varying displacement of the bob from its rest position is permanently recorded on a paper chart by a repetitive high-voltage spark occurring at the position of the bob. An instantaneous indication of acceleration is also obtained since the record paper is visible through the transparent front of the accelerometer case immediately after puncture.

---

* Communicated by the Director.

[1] For more complete details, see "A Novel Recording Accelerometer," by A. S. Iberall, *Rev. Sci. Inst.*, Vol. 20, p. 304 (1949).

V.2
194

The accelerometer constructed at the Bureau is built into a rate-of-climb indicator case of the standard aircraft-panel type. By means of the zero-setting shaft of the rate-of-climb indicator, power from a small synchronous timing motor for driving the record chart is transmitted from the back to the front of the case without obstructing the available space. Sprocketed rollers mounted just behind the front of the case are thus made to pull the recording paper across the inner face of the cover and push it out the side of the case, where it may be torn off. As the recording paper passes across the face of the instrument, it is punctured by sparks at a 60-cycle repetition rate. The writing electrodes consist of a nickel tip projecting perpendicularly from the bob, and the edge of a narrow strip mounted on the inside of the cover directly under the tip. The bob and nickel tip are made the high-voltage electrode while the plate and other parts are grounded to permit removal of the cover without risk of electrical shock. The high voltage is provided by a small model-airplane spark coil mounted behind the motor. Current is brought to the bob through insulated banana plugs so that removal of the cover for loading the record will cut off the voltage to the electrodes.

The linear speed of the record chart is about 6 inches per minute. The cartridge for storage of the record chart is mounted in a semi-cylindrical depression in the outside of the transparent plastic cover, which is slotted to received the tangent lip of the cartridge.

A 35-mm. single-weight perforated photographic paper with no emulsion was chosen for the record chart. As the thickness of the paper (0.005 in.) required more energy to form an easily visible trace than was available from the small spark coil, a simple preliminary chemical treatment was developed for the paper to intensify the trace as it formed.

The necessity of operating the accelerometer aboard a plane from a 28-volt source of direct current also required the development of a special power supply. A 60-cycle vibrator is employed in the usual way to produce 60-cycle alternating current for the motor. However, the power dissipation of the small spark coil makes operation by a repetitive voltage "pip" most desirable. This pip is supplied by the inductive decay of the vibrator coil on the "break" of its main reed contact.

In laboratory performance tests at the National Bureau of Standards, the accelerometer successfully withstood shock and vibration of at least 15 *g* units of acceleration. Paper speed was found uniform to within a few per cent. The record obtained was easily interpreted and adequate for resolving detail of amplitude not less than 2 per cent of the total record width.

THE FRANKLIN INSTITUTE LABORATORIES FOR RESEARCH AND DEVELOPMENT

Abstract of **An A-c. System of Remote Indication and Its Application to the Measurement of Fluid Pressure and Flow.**[1]—HOWARD D. WARSHAW.[2] A moving-vane indicator in circuit with a two-coil transmitter forms a system of remote indication relatively free from errors due to variations in ambient temperature, supply voltage, and supply frequency. The transmitter is simple and should withstand severe vibration and extreme temperatures. The electrical elements of the transmitter are completely isolated from the mechanical components so that measurements in the presence of corrosive or explosive fluids may be made with safety. Applications are presented in which the transmitter measures oil pressure in the crankcase of a gasoline engine and the flowmeter measures fuel flow. This system of remote indication has been developed for use in aircraft, but its potentialities for industrial applications will become evident. The experimental models were designed to operate from 400-cycle aircraft power sources; larger components would be required for 60-cycle operation.

The transmitter contains a movable core within a set of coils which are connected so that their magnetic fields are in opposition. The core is displaced by a force derived from the fluid under measurement, and its position is established when the fluid force is balanced against the opposing force of a coil spring. Three conductors serve to transmit two electrical signals from the transmitter to the indicator.

The indicator contains a vane of highly permeable magnetic material located within a set of crossed coils. The transmitter voltages are applied to the indicator coils through a bridge circuit, and their resultant magnetic field positions the vane which is fastened to the pointer shaft. The indicator contains resistors for sensitivity and end-scale adjustments, and suitable assemblies for damping and pointer zero return.

One application of this system is to the electrical remote indication of aircraft engine oil pressure. There is a need for an aircraft remote-reading oil-pressure gage with a transmitting element suitable for direct mounting on the aircraft engine. The coagulation, at low temperatures, of the engine oil in the line from the crankcase to the transmitter of any of the remote-indicating oil-pressure gages in present use makes these gages inoperative during a part of the engine warm-up period. The lack of oil pressure indication at this time frequently leads to serious engine damage which would not otherwise occur. The device herein described is capable of offering a satisfactory solution to this problem.

Models of both transmitter and indicator for measuring oil pressure are shown in Fig. 1. Figure 2 shows the same transmitter partly disassembled.

Another application of this system is to the remote indication of fluid rate-of-flow through tubing such as the fuel supply line of an aircraft engine. One model of the flowmeter transmitter is shown in Figs. 3, 4.

Electromagnetically, the operation of the flowmeter transmitter is identical to that of the pressure transmitter. The difference lies in the hydraulic system used to derive the force necessary to displace the core. In this application, the magnetic core is tubular, and is designed to support firmly an orifice plate that restricts the flow of fluid. The restriction sets up

[1] Paper published in *Instruments*, Vol. 22, p. 402 (1949).

[2] Research Engineer, The Franklin Institute Laboratories for Research and Development, Philadelphia, Pa.

a pressure differential across the orifice plate that positions the core against the restraining force of a coil spring. Figure 4 shows the core with one orifice plate installed, and Fig. 3 shows two replacement plates that are used for different ranges of rate-of-flow.

The pressure gage was tested to determine the inherent inaccuracies of the electrical system.

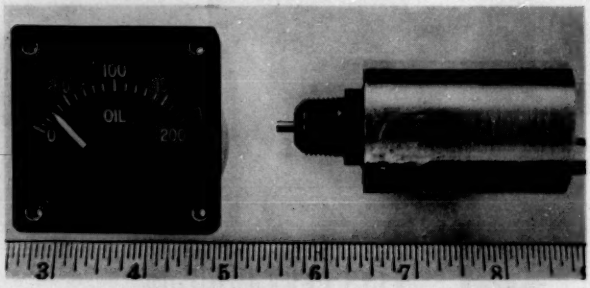

FIG. 1. Pressure transmitter and indicator.

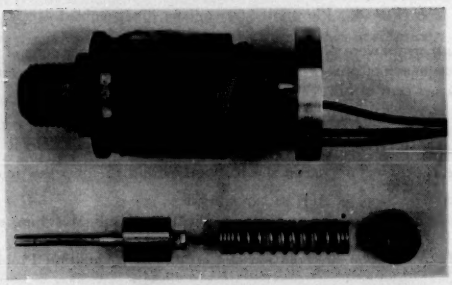

FIG. 2. Pressure transmitter disassembled.

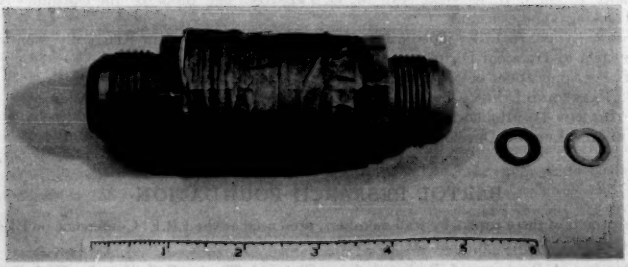

FIG. 3. Flowmeter transmitter.

With the indicator at room temperature (25 deg. C.) the transmitter temperature was varied from minus 55 deg. C. to plus 70 deg. C. The maximum error in indication was approximately plus-or-minus two per cent of full scale. When the supply voltage was varied from 80 to 120

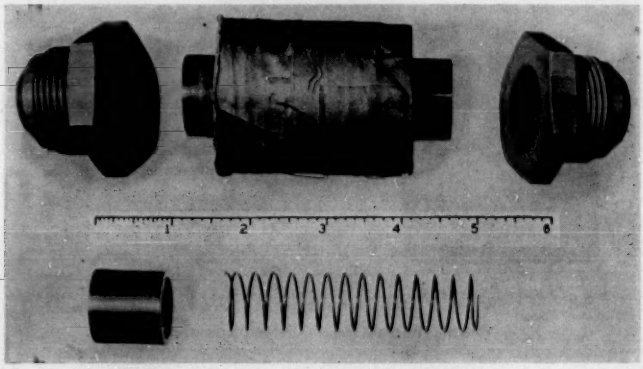

FIG. 4. Flowmeter transmitter disassembled.

volts, the maximum errors were plus 0.3 per cent and minus zero per cent of full scale. Variations in supply frequency of plus-or-minus 5 per cent produced maximum errors in indication of plus-or-minus 1 per cent of full scale.

JOURNAL OF THE FRANKLIN INSTITUTE

The following papers will appear in the JOURNAL within the next few months:

COULSON, THOMAS: The Story of Aids to Navigation.

FANO, ROBERT M.: Theoretical Limitations on the Broadband Matching of Arbitrary Impedances.

FANO, ROBERT M.: A Note on the Solution of Certain Approximation Problems in Network Synthesis.

LUCKIESH, MATTHEW, A. H. TAYLOR, THOMAS KNOWLES AND E. T. LEPPELMEIER: Inactivation of Molds by Germicidal Ultraviolet Energy.

MECHLER, E. A., J. B. RUSSELL AND M. G. PRESTON: The Basis for the Optimum Aided-Tracking Time Constant.

JACOBSEN, LYDIK, R. L. EVALDSON AND R. S. AYRE: Response of an Elastically Non-Linear System to Transient Disturbances.

YU, Y. P.: Applications of Network Theorems in Transient Analysis.

MOON, PARRY AND DOMINA EBERLE SPENCER: A Modern Approach to Dimensions.

GRIFFITH, ROY T.: Minimotion Typewriter Keyboard.

SILBERSTEIN, LUDVIK: Developable and Developed Silver Halide Grains.

BARTOL RESEARCH FOUNDATION

Abstracts of three papers by staff members, presented at the I.R.E. Conference on Electron Devices held at Princeton, June 20–21, 1949.

Decay and Recovery of Emission from Sintered Thoria Cathodes in High-Vacuum Diodes, by DANIEL L. GOLDWATER. A variety of phenomena involving time-changes of

emission from sintered thoria cathodes have been explored. The results were discussed with reference to separation into three components: one steady state and two changing. Order of magnitude values of various parameters were presented and discussed briefly with reference to possible applications of this type of cathode.

Rate of Evaporation of Thoria, by EDWARD M. SHAPIRO. The rate of evaporation of thoria from thoria-coated filaments as a function of temperature was measured in the range 1700–1950° C_{B_r}. Vapor pressures calculated from the evaporation rates were compared with vapor pressures measured by the effusion method. In addition some studies of evaporation rates with emission were discussed.

Radiation Transfer Considerations in the Heating of a Cathode Sleeve, by W. E. DANFORTH. The theory of radiation heat transfer was briefly developed with particular reference to cathode heating. Experiments were described in which metal and ceramic sleeves were heated by an internal cylindrical radiation. The observed temperatures were discussed in relation to the thermal emissivities of the several surfaces.

Abstract published in the *Bulletin* of the American Physical Society's meeting in Cambridge, Mass, June 16–18, 1949.

Radiations from Indium (114) and Barium (140),* by C. E. MANDEVILLE[1] AND E. SHAPIRO.[1] The 72-Second In^{114} activity, in equilibrium with its 48-day isomeric parent, was induced in metallic indium irradiated by slow neutrons in the Oak Ridge pile. Chemical separations were performed for the removal of Ag, Ca, Cu, Fe, Ni, and Pb as possible impurities. The beta-rays have a maximum energy of 1.89 Mev as measured by aluminum absorption, and the maximum gamma-ray energy is 0.90 Mev as determined by coincidence absorption. A lead absorption curve gives quantum energies of 0.15 Mev and 0.70 Mev. Beta-gamma coincidence data show that the harder gamma-rays are associated with less than 5 per cent of the nuclear beta-rays. A gamma-Gamma-coincidence rate of 0.25×10^{-3} coincidence per gamma-ray was noted. Fission-produced Ba^{140} emits beta-rays of maximum energy 0.91 Mev. Lead absorption curves observed continuously for 90 hours during growth of La^{140} reveal the presence of 0.14 Mev and 0.6 Mev quanta emitted by Ba^{140}. Beta-gamma coincidence measurements show that the beta-spectrum of Ba^{140} is complex.

* Assisted by the joint program of ONR and AEC.

[1] Bartol Research Foundation of The Franklin Institute, Swarthmore, Pa.

The Maximum Range of High Energy Electrons in Matter.—F. L. HEREFORD[1] AND C. P. SWANN.[1] Investigations of the penetration of high energy electrons in matter are of considerable interest because of the widespread use of absorption measurements in the determination of beta and gamma ray energies. Information concerning electron scattering also finds ready application in this connection. In the absence of experimental data for electrons of energy exceeding 3 Mev. we have undertaken an investigation of these matters in the energy range from 3 to 12 Mev. The beta rays from B^{12} are being employed as a source, the production of B^{12} being attained through the B^{11} (d,p) B^{12} reaction with the Bartol Van de Graaff machine.

An electron beam homogeneous in energy is obtained by analysis of the B^{12} beta ray spectrum with a 90° magnetic spectrometer. Using a triple coincidence train of Geiger-Mueller counters absorption curves of this beam have been determined at various energies. Extrapolation of the linear portion of the curves through the zero intensity axis yields range values which may be compared with existing computed values,[2] the range so determined corresponding to the so-called "practical maximum range." Results obtained thus far with aluminum absorbers[3] have indicated experimental values somewhat less than the computed values.

It seems probable that this discrepancy can be due to multiple scattering effects which would yield actual ranges greater than the measured absorber thicknesses. Energy loss through

radiation is also effective at these energies. However, for moderate energies (60 Mev.) in aluminum most electrons will not experience radiative collisions; hence, their maximum range will be unaffected.

Since both radiation and scattering depend heavily upon the atomic number of the absorber, it is hoped that measurements employing heavier elements will throw some light on the question. Preliminary results obtained with copper have indicated that maximum range values determined by the method employed are definitely dependent upon scattering effects (and hence counter geometry) to a sufficient extent to account for the discrepancy mentioned above. Further work is continuing with the aim of obtaining experimentally defined maximum range values which may be of use in absorption measurements in the high energy region.

[1] Bartol Research Foundation of The Franklin Institute, Swarthmore, Pa.

[2] W. A. FOWLER, C. C. LAURITSEN AND T. LAURITSEN, *Rev. Mod. Phys.*, **20**, 237 (1948).

[3] *Phys. Rev.*, Aug. 15, 1949.

LIBRARY

The Committee on Library desires to add to the collections any technical works that members would wish to contribute. Contributions will be gratefully acknowledged and placed in the library. Duplicates received will be transferred to other libraries as gifts of the donor.

Photostat Service. Photostat prints of any material in the collections can be supplied on request. The average cost for a print 9 × 14 inches is thirty-five cents.

The Library and reading room are open on Mondays, Tuesdays, Fridays and Saturdays from 9 A.M. until 5 P.M.; Wednesdays and Thursdays from 2 P.M. until 10 P.M.

RECENT ADDITIONS

ASTRONOMY

HOSMER, GEORGE L. Practical Astronomy. Ed. 4. 1948.

CHEMISTRY AND CHEMICAL TECHNOLOGY

GREGORY, C. H. AND OTHERS. Instrumentation and Control in the German Chemical Industry. 1947.

INTERNATIONAL COMMITTEE ON NEW ANALYTICAL REACTIONS AND REAGENTS. Reagents for Qualitative Inorganic Analysis. 1948.

MARTIN, L. H. AND HILL, R. D. A Manual of Vacuum Practice. 1947.

ELECTRICITY AND ELECTRICAL ENGINEERING

KIMBARK, EDWARD WILSON. Electrical Transmission of Power and Signals. 1949.

ROBERTSON, BURTIS LOWELL AND BLACK, L. F. Electric Circuits and Machines. 1949.

FOOD

BRAUERMAN, J. B. S. Citrus Products. 1949.

GEOLOGY

NEVIN, CHARLES MERRICK. Principles of Structural Geology. 1949.

INDUSTRIAL MANAGEMENT

BARNES, RALPH MOSSER. Motion and Time Study. 1949.

RUTHERFORD, JOHN G. Quality Control in Industry. 1948.

MATHEMATICS

CARATHEODORY, CONSTANTIN. Reelle Funktions. Volume 1. 1946.

MCLACHLAN, N. W. Modern Operational Calculus. 1948.

TODD, JOHN ARTHUR. Projective and Analytical Geometry. 1947.

MECHANICAL ENGINEERING

BUNDY, F. P., EAGAN, T. E. AND BOYER, RALPH L. Wear, as Applied Particularly to Cylinders and Piston Rings. 1948.
GRODZINSKI, P. AND JACOBSOHN, W. Diamond Tool Patents. 3 parts. 1945–1948.
REIBEL, SIDNEY. Trolley Conveyors. 1949.

METALLURGY

INSTITUTE OF METALS. Symposium on Internal Stresses in Metals and Alloys. 1948.
SIMPSON, BRUCE L. Development of the Metal Casting Industry. 1948.
STANSEL, N. R. Induction Heating. 1949.

MINING ENGINEERING

HOOVER, THEODORE JESSE. The Economics of Mining. Third Edition. 1948.

PHYSICS

GURNEY, RONALD W. Introduction to Statistical Mechanics. 1949.
HOWE, HARLEY EARL. Introduction to Physics. Second Edition. 1948.
MEYER, CHARLES FERDINAND. The Diffraction of Light, X-rays and Material Particles. 1949.
Nuclear Fission and Atomic Energy. 1948.

PLASTICS

DELMONTE, JOHN. Plastics in Engineering. 1949.

RADIO

HUPERT, J. Radio Communication Transmitters. 1948.

TEXTILES

LEGGETT, WILLIAM F. The Story of Silk. 1949.
TEXTILE INSTITUTE. Identification of Textile Materials. No date.

WOOD

BROWN, H. P.; PANSHIN, A. J. AND FORSAITH, C. C. Textbook of Wood Technology. Volume 1. 1949.
GLESINGER, EGON. The Coming Age of Wood. 1949.
TITMUSS, F. H. A Concise Encyclopedia of World Timbers. 1949.

MUSEUM

"Is that a demonstration of perpetual motion?" ask scores of museum visitors who peer down the main stairwell at the gently swinging 1800-lb. bob of the Foucault pendulum. Anyone who witnessed the extraordinary parade which heralded the installation of the pendulum might have been justified in supposing it had some such momentous purpose. Surrounded by a mounted police escort, eleven sturdy men were strung out over a length of 85 feet, each holding on to a slender bronze wire only one quarter inch in diameter. Not that the wire was any great weight, it weighed only nine pounds, but it was essential that no kinks form in the wire.

The pendulum is an impressive sight, the 1800-lb. shot-filled ball swinging at the end of an 85-ft. suspension. Its periodical swing is a visual demonstration of the Earth's daily rotation.

The issue of the JOURNAL for May, 1851, contains the translation of a paper by Jean Bernard Leon Foucault, the eminent French physicist, who had hung a similar pendulum from the dome of the Pantheon in Paris. In his paper Foucault describes the purpose of the pendulum, which was to furnish a physical demonstration of the Earth's rotation without any reference to a point beyond the Earth. The significance of the paper appears to have been realized

by the members of the Institute, because the following six months produced communications from three of them relating to the pendulum.

The pendulum is set swinging in a north-south direction each day at a predetermined time. An observer will perceive that at the end of an hour the compass dial beneath the swinging bob has rotated nearly ten degrees. Each successive hour reveals that a similar change has taken place. The impression gained is that the pendulum itself changes the direction of its motion, but this is not true.

The physical property of a swinging pendulum is that once it has been started swinging in a particular plane, the pendulum will maintain that plane, and so it might be considered an invariable plane of reference.

The Earth is a spinning body which rotates once in twenty-four hours. Consequently, a body on the equator of the Earth is carried around with a linear speed of about 1000 miles an hour. In our latitudes the linear speed of a body is about 750 miles an hour, while at the north pole the linear speed is zero. As a result, in the northern hemisphere a body south of us has a higher linear speed than we have and, likewise, we have a higher speed than a body north of us. Thus, if we are in a room the south end of the room will travel faster than the north end—the room will rotate.

Combine the two motions of the pendulum in a plane and the rotation of the room due to the rotation of the Earth and we see the compass dial turning under the pendulum.

To appreciate how the pendulum maintains its uniform motion, independent of the roof from which it is suspended, it is advisable to descend to the stair foot where a model of the pendulum and its unique suspension is displayed and may be operated.

The principle may be visualized further by thinking of a merry-go-round in which the animals represent the compass points. Imagine a pendulum suspended at its center. While the merry-go-round stands at rest the pendulum is set swinging in the direction of a stationary spectator. Then the merry-go-round is set turning. The pendulum will continue to swing in the direction of the spectator. But one after another the animals will pass it in succession, and to a rider on the merry-go-round the pendulum will appear to be changing the direction of its swing.

If it were possible to suspend a pendulum immediately over the north pole it would act as in the merry-go-round analogy, it would change its apparent direction 15 degrees every hour. On the other hand, at the equator the Earth turns in a plane perpendicular to that at the pole and the Foucault pendulum would show no change in direction because the Earth is not actually turning under it. The degree of motion increases the farther north one proceeds. At the latitude of Philadelphia the Earth turns through 9.6 degrees every hour.

The Institute's pendulum does not have the longest suspension which has been used to demonstrate this principle. Experiments in Rheims and Amiens cathedrals (the latter with a suspension of 165 ft.) exceeded its length. But the entire setting, the gleaming 23-in. steel shell filled with small shot, the simple yet beautiful compass dial, and the convincing model, constitute a notable tribute to the public spirit of the donors, Mr. and Mrs. Richard L. Binder.

NOTES FROM THE BIOCHEMICAL RESEARCH FOUNDATION

ABSORPTION OF ULTRA-VIOLET LIGHT BY LIVING CELLS *

BY

J. O. ELY AND M. H. ROSS

Nucleic acids, because of the presence of purines and pyrimidines in the molecule, absorb ultra-violet light with a maximum absorption at 2600 Å. Recently, Larionow and Brumberg (1) suggested, on the basis of ultra-violet light photomicrographic studies, that desoxyribonucleic acid, as it exists in the nuclei of living cells, does not absorb ultra-violet light of wave-lengths near 2600 Å. These investigators contended that absorption develops as a result of injury or death of the cell.

Ultra-violet light photomicrographs of living cells made in this laboratory show absorption of light of wave-length 2654 Å. Cells of the Walker Carcinoma No. 256 of the rat were used. Cell suspensions

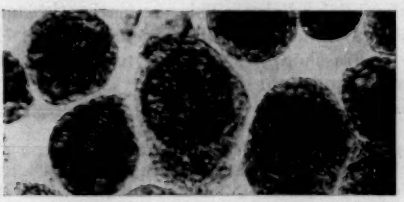

Ultra-violet light (2654 Å) photomicrograph of Walker Carcinoma No. 256 of the rat, magnification 900 ×.

were prepared immediately after removal of tumours from the host by mincing tissue finely with scissors in Ringer's solution and straining through a thin layer of cotton to remove coarse aggregates. Cells prepared in this manner and kept for much longer periods of time than was required in these experiments produced tumours when implanted into rats. The cells, in Ringer's solution, were placed on a quartz slide and covered with a quartz coverglass and sealed with paraffin.

Ultra-violet light photomicrographs were made with a quartz optical system microscope by the method previously described (2), with a 2.5 mm. objective, N. A. 0.85 and a 10 × ocular, magnification 240 ×. Condenser diaphragms were closed to small aperture.

* Reprinted from *Nature*, Vol. 163, p. 906, June 11, 1949.

Focusing was performed by means of a fluorescent screen and a magnifier with 2654 Å light. The focus was obtained on one area of the field; all light was then barred from the microscope, and the slide was moved to a distant field. In this procedure the cells were exposed to only the amount of ultra-violet light necessary to produce the image on the film. Panatomic X (Eastman Kodak Co.) was used. Photomicrographs made in this manner (see illustration) show the same absorption pattern as those made after the cells have been exposed to several times the amount of ultra-violet light necessary for photomicrographs.

Nuclear and cytoplasmic absorption varied considerably from cell to cell, depending on the metabolic state. Chromosomes, where present, absorbed intensely. In the resting cells the nucleolus usually absorbed much more intensely than did the remainder of the nucleus.

Visual observations of fluorescent images of cells illuminated by ultra-violet light made by rapidly moving the slide across the microscopic field revealed absorption by cells as they came into view; under these conditions exposure to ultra-violet light was less than one second. Chicken erythrocytes in whole blood when observed in this manner within three to five minutes after drawing the blood showed intense nuclear absorption. These observations, which have been repeated many times, indicate that the nucleic acids as they exist in the living cells absorb ultra-violet light. This contention is supported by the work of Wyckoff (3), who made successive ultra-violet (2750 Å) photographs of a living grasshopper spermatocyte and showed absorption by the chromosomes throughout division.

REFERENCES

(1) L. T. LARIONOW AND E. M. BRUMBERG, *Nature*, **158**, 663 (1946).
(2) J. O. ELY AND M. H. ROSS, JOUR. FRANKLIN INST., **246**, 87 (1948).
(3) R. W. G. WYCKOFF, "Symposia on Quantitative Biology," **2**, 39 (1934).

BOOK REVIEWS

INDUSTRIAL RHEOLOGY AND RHEOLOGICAL STRUCTURES, by Henry Green. 311 pages, illustrations, 14 × 22 cm. New York, John Wiley & Sons, Inc., 1949. Price, $5.50.

This book is neither a reference book nor a textbook. It is a highly readable distillation of the late Henry Green's experiences as a rheologist, microscopist, and industrial researcher. The book is intended to guide "Bill," an industrial investigator, into the field of rheology, and its primary purpose is to present Bill with a workable rheological system based on accepted principles, rigorously demonstrated. The organization of the book is intended to further this purpose. Part I, A Rheological System, defines Newtonian, Bingham and "pseudoplastic" flow, and discusses the measurement, calculation and meaning of viscosity, yield value, plastic viscosity and thixotropy. It describes the various types of flow and the various systems which have been proposed to measure them. Based on this very clear review of rheological science, Mr. Green constructs a rheological system for the evaluation of Newtonian liquids and Bingham bodies. Part II, The System Applied to Laboratory Measurements, is most complete in its description of the calibration and use of the rotational viscometer and the tackmeter. Some other types of viscometers are mentioned but not described in detail. Further conceptions regarding the types of flow exhibited by various materials are presented and materials are described whose behavior illustrates the principles stated in Part I.

Part III, The Particle—The Basis of Rheological Structure, discusses the role of suspended particles in determining the flow properties of a material. It is chiefly concerned, however, with the measurement of particle sizes with the white light, ultraviolet and electron microscope. This relatively short section (40 pages) is well worth the attention of anyone who desires to examine particles in a liquid suspension. The JOURNAL OF THE FRANKLIN INSTITUTE published two of Mr. Green's original papers on the microscopy of pigment particles, in 1921 and 1927.

Part IV, Particle Groups and Rheological Structures, integrates the conceptions of Parts I and III to explain the causes and formation of structure in suspensions and colloids. This section includes the following types of materials: Newtonian, Pseudoplastic, Dilatant, Plastic, Brittle, Thixotropic, Two-Dimensional Flocculates, and Artifacts. The inclusion of photomicrographic and optical evidence to account for flow properties is a unique and valuable feature of this presentation. Structure is explained in terms of the flocculation of the particles present.

The book contains nine appendices which include supplementary information on instrument corrections and use, and advice to Bill and to Bill's boss, the Laboratory Director. A glossary, bibliography and indices are included.

This book, the fruit of thirty years of investigation by one of this country's outstanding rheologists and microscopists, presents for the first time, to quote the jacket, "the unique scientific correlation of rheological with microscopical investigations." This relatively novel approach commends the book to practicing rheologists, even though the book also successfully fulfills its primary purpose of giving Bill a practical rheological system. The rheological system that Mr. Green presents reflects his special interest in printing inks, paints, varnishes, oils and other low-consistency materials, and an investigator in these fields can use Mr. Green's system readily.

The system is not intended to be useful for the investigation of high-consistency materials such as resins, asphalts, rubber and industrial plastics. In fact, Mr. Green considers that no "industrially-useful" system for such materials can be recommended at present because no way is yet known for describing their flow properties independently of such experimental variables as rate of shear or shearing force. The various power equations that have been introduced for evaluating the flow of such materials are dismissed as mathematical methods of curve-fitting, devoid of real physical significance. The evaluation of elasticity, so necessary

for characterizing high-consistency materials, is barely mentioned. The possible role of selective adsorption in the formation of liquid layers around the solid particles is not mentioned, even though this conception is useful in explaining thixotropy, aging and adhesion of high-consistency heterogeneous materials.

In summary, this book is an important compilation and correlation of rheological principles and microscopic phenomena. It presents a rheological system that can be applied readily to investigations of the flow properties of low-consistency materials. Although it presents much which is of interest to workers with high-consistency materials, such investigators will have to look elsewhere for methods and conceptions unique to their problems or useful in their solution.

E. THELEN

MAGNETIC RECORDING, by S. J. Begun. 242 pages, drawings and photographs, 15 × 23 cm. New York, Murray Hill Books, Inc., 1949. Price, $5.00.

This is one of the first full-length books devoted exclusively to magnetic recording. It includes in an elementary fashion a large variety of material dealing with the history and theory of magnetic recording, properties of magnetic materials and examples of much modern apparatus. The volume is profusely illustrated with photographs of commercial magnetic recording equipment manufactured by all of the major producers. By providing this survey of equipment made to-day it shows the design manifestations of the engineering problems peculiar to magnetic recording techniques. Circuit diagrams showing values are provided for most of the sets.

The equipment and diagrams occupy approximately one half of the book. The other half is devoted to the presentation of simple conceptions of sound, magnetism, magnetic materials and induction principles. The treatment is similar to that used by J. F. Rider, the technical content being at the radio serviceman's level.

The elementary nature of the book is emphasized by the care taken to describe what is meant by such terms as "wavelength," "period," etc. The style of writing is informal. Each chapter is followed by a liberal bibliography. It is also interesting to note that a list of patents is given, and this may be extremely valuable to certain readers.

The lack of fundamental information such as might be derived from a thorough research program on the many phases of magnetic recording is surprising in the light of the author's affiliation (Vice-President and Chief Engineer, The Brush Development Co.). Such information must have been available to him, and it is certain that, unless the competitive nature of the industry prevented his publishing such data, the book could have been far less dated and infinitely more useful in the engineering field. Owing to the broad applicability of magnetic recording to communications and especially to the process of information storage in large-scale, high-speed computing equipment, the subject has far greater significance than "a challenge to the phonograph."

C. W. HARGENS

OUR SUN, by Donald H. Menzel. 326 pages, illustrations, 15 × 22 cm. Philadelphia, The Blakiston Co., 1949. Price, $4.50.

This is the long-awaited, eighth volume of the Harvard Books on Astronomy, and is in every way worthy to rank with the other seven. The author explains that its publication was prevented during the war years and until now by military censorship, because of the chapters on Solar Chemistry and Atomic Energy.

The style of the writing is very clear and easily understood. Difficult mathematics is largely omitted, and where necessary, is explained by drawings and simple illustrations. The wealth of photographs is one of the most delightful parts of the book.

The chapters on Sunspots, Prominences and Fine Details of the Solar Surface give more information than we have ever had before. The chapter on Eclipses gives abundant details of the phenomena and the methods of observing them.

The author is particularly pleasing in his brief summary of the origin of life and the course of evolution in its relation to solar energy, and his last chapter, called The Sun and You, gives

serious but practical thought to the future when the sources of energy that we use now will be exhausted and to the possibility of using the direct energy of sunlight.

Altogether the book is fine, and it will be enthusiastically welcomed by readers of the former volumes. It ought to make new friends for the whole series.

WILLIAM L. FISHER

PHOTOELASTICITY AND ITS APPLICATION, by V. K. Zworykin and E. G. Ramberg. 494 pages, illustrations, 15 × 24 cm. New York, John Wiley & Sons, Inc., 1949. Price, $7.50.

This volume replaces the earlier work by Zworykin and Wilson entitled "Photocells and Their Application," the second edition of which was published at a time when many of our currently useful devices were still in their infancy. In common with the previous work, the authors once again authoritatively present practical data as well as the physical properties of modern photoelectric devices, with a minimum of detailed physical theory and mathematical development.

The twenty chapters of this book can be roughly divided into two major groups, those pertaining to the principles and preparation of photo-sensitive devices and those pertaining to the application of such devices. An historical introduction acquaints the reader with the three common photoelectric effects: photovoltaic, photoconductive, and photoemissive; and the early experiments which led to their discovery. This chapter is followed by one which discusses the general theory of radiant and thermal energy and the basic principles of the photoemissive effect.

The special characteristics looked for in phototubes are dependent upon the physical and chemical treatment given to the emissive surfaces, which are usually derived from thin alkali films on a metal base. These are described, again with reference to the latest experiments, with numerous graphs showing the sensitivities of a wide variety of surfaces.

The modern materials, apparatus, and practical methods followed in making phototubes are described for the cases of the: vacuum, gas-filled, multiplier, and image phototubes, and photoconductive and photovoltaic cells. The physical and electrical characteristics of each of these classes of tubes are described in a logical and continuous manner, starting with the simplest type and going on to the more complex means of amplification. Detailed explanations of recent basic findings supplant discussions of their operating characteristics.

The remaining nine chapters are devoted to applications of photoelectric devices, from the common and simple trigger relay to the more complex and physically more interesting field of infra-red detection. Basic circuits for light measurement and light activation are examined and many practical auxiliary electronic circuits are described utilizing a wide variety of available phototubes. When small photo currents are to be measured, consideration must be given to the many types of noise which ultimately limit the smallest light signal which can successfully be detected. One chapter is devoted to this interesting subject.

Descriptions of many industrial applications which use one form or another of the phototube as a scientific tool include the following: photometry, reflectometers, spectrophotometers, sound reproduction, television picture transmission including facsimile, flying spot and ultrafax, television camera tubes, light beam signaling, infra-red detection, industrial process controls, and others.

The broad fields considered by the authors allow the reader who specializes in any one of many scientific branches to apply the practical information to his own experimental work. While not written as a formal textbook, both practicing engineers and students should profit from the book as a useful tool, not only because of its own content, but because of the hundreds of references, listed throughout the work. It should find its way into the technical libraries of many serious investigators.

S. CHARP

ERRATUM: The August JOURNAL incorrectly listed the publisher of "Principles of Electricity and Electromagnetism," by Gaylord P. Harnwell. The book is published by McGraw-Hill Book Co., New York.

BOOK NOTES

ELECTRIC RESISTANCE STRAIN GAUGES, by W. B. Dobie and P. C. G. Isaac. 114 pages, illustrations, diagrams, 14 × 23 cm. London, English Universities Press, Limited, 1948. Price, $3.50 from Macmillan Company, N. Y.

Among the newer tools which have proved their value to the research engineer are electric resistance strain gauges. Messrs. Dobie and Isaac have written this compact summary on the subject, based on a wide perusal of the pertinent literature. The various types of gauges are described and a long table gives the characteristics of the various commercial types. The determination of static strain, and stress analysis are both treated at some length. Other chapters provide the necessary elementary electronics and discuss electronic bridge circuits. Numerous applications of strain gauges have been located by the authors and are described briefly. Extensive bibliographical references are given for those who wish to refer back to the original sources.

DIFFERENTIAL EQUATIONS, by Harry W. Reddick. Second edition, 288 pages, figures, 14 × 21 cm. New York, John Wiley & Sons, Inc., 1949. Price, $3.00.

This textbook, limited to ordinary differential equations, appears now in a revised second edition. The author has taken the opportunity of rewriting parts of the text as well as adding a new chapter on the linear equation of second order. Additional problems have been added and answers are provided for all.

CONVEYORS AND RELATED EQUIPMENT, by Wilbur E. Hudson. Second edition, 468 pages, illustrations, tables, 15 × 23 cm. New York, John Wiley & Sons, Inc., 1949. Price, $7.00.

Newer methods of handling materials are reflected in this revised edition of Hudson's work. The use of pallets and skids with trucks and tractors is discussed, while additional data have been supplied on the subjects of pneumatic conveyors and belts. Two new chapters have been added, one dealing with special problems and their solutions, and the other with the increasing number of dust-explosion hazards that are encountered in materials handling. With the revisions it continues to be a useful work in the field.

DESIGN OF MACHINE ELEMENTS, by M. F. Spotts. 402 pages, diagrams, tables, 15 × 23 cm. New York, Prentice-Hall, Inc., 1948. Price, $6.65.

In the art of machine design it is necessary to know the fundamental principles involved in the design of the various elements of which a machine is composed. This textbook is limited to a consideration of these machine elements, the material being so developed that the chapters are independent of each other and may be studied in any order. A preliminary chapter considers fundamental principles while concluding chapters discuss Dimensioning and Details, and Engineering Materials. Problems, bibliographies and tables of properties of engineering materials are features of the book.

TABLE OF SINES AND COSINES TO FIFTEEN DECIMAL PLACES AT HUNDREDTHS OF A DEGREE, by National Bureau of Standards. 95 pages, 20 × 29 cm. Applied Mathematics Series 5. Washington, D. C., Government Printing Office, 1949. Price, $0.40 (paper).

This new table of sines and cosines with decimal divisions of a degree has been issued to meet the need for a high-accuracy table of this type. The columns of sines and cosines are arranged side by side for the benefit of those needing both functions for the same argument. Another of the many valuable tables being prepared by the Computation Laboratory of the National Applied Mathematics Laboratories.

CURRENT TOPICS

Seek Cosmic Ray Secrets in Far North Research.—An expedition of American scientists is seeking new clues to the secrets of cosmic ray activity at 20-mile altitudes, near "the top of the atmosphere," over the Canadian outpost settlement of Churchill on the shore of Hudson Bay.

The project is being sponsored jointly by the National Geographic Society and the Bartol Research Foundation of The Franklin Institute, Swarthmore, Pennsylvania. The National Defense Board of Canada is cooperating in the undertaking. It is part of a continuing program of cosmic ray research instituted in 1946 by the two sponsors and supported by the Air Force and the Office of Naval Research.

A major objective of the expedition is to develop experimental evidence whether the sun is surrounded by a constant magnetic field similar to that possessed by the earth. There is considerable scientific controversy on this subject.

Test For Theory

Dr. Martin A. Pomerantz of the Bartol Foundation, who heads the expedition, believes that a study of cosmic ray behavior at high altitudes in the Far North may lead to the answer for this riddle.

Data pointing to the importance of the project resulted from previous experiments conducted as far north as 52 degrees geomagnetic latitude and at altitudes of 30,000 ft., utilizing specially equipped B-29's. The geomagnetic latitude of Churchill, Manitoba, is roughly 69 degrees north (ten degrees greater than the more familiar geographic latitude), and this research program is being conducted at heights in excess of 100,000 ft., or more than three times the altitudes possible in the B-29 tests.

The theory under test is that cosmic rays should increase in intensity as the North Pole is approached, since one is moving farther away from the equator where the earth's magnetic field is the strongest.

However, if the sun possesses a magnetic field of sufficient magnitude, its effect would be superimposed on that of the earth's magnetic field. In that event, the intensity of these primary rays would remain constant north of a particular latitude.

To Use Geiger Counters

Geiger counters, the now familiar atomic age instrument for reporting radioactivity, are doing the high altitude detective work for the scientists in a number of free-balloon flights.

Each flight takes aloft a four-fold coincidence arrangement of Geiger counters. This arrangement, Dr. Pomerantz explained, acts something like a telescope in the sense that it produces a signal whenever a cosmic ray particle goes through in a certain direction.

All data are continuously transmitted by radio to a receiving station on the ground. Information regarding the atmospheric pressure, and hence the

altitude, the temperature within the apparatus, and cosmic ray intensity, likewise are received throughout the duration of the flights and recorded on a moving paper tape. A special trailer serves as the party's mobile laboratory.

Weather A Factor

In directing the program, Dr. Pomerantz will be assisted by two colleagues from the Bartol Foundation, Robert J. Kerr, and Robert C. Pfeiffer, both of Swarthmore, Pennsylvania. Dominion authorities promise that additional assistance will be provided by Canadian meteorological personnel stationed at Churchill, now the location of a defense installation.

Dr. Pomerantz and his party left for Churchill about August 1, and hoped to complete their program of field work in a month.

The August period was selected because it usually has the most favorable weather conditions for the work at the Canadian outpost—minimum surface winds at sunrise when the instrument-laden balloons will be launched, and very light precipitation.

Waning Rays Noted

Previous research has established that primary cosmic ray particles (those impinging upon the top of the earth's atmosphere) are affected by the earth's magnetic field when they arrive from an as yet undetermined source or sources in outer space. In fact, the earth acts like a huge mass spectrograph in separating particles of different energies.

This phenomenon gives rise to what is called the latitude effect. As one proceeds toward the equator, strongest zone in the earth's magnetic field, the rate at which cosmic particles arrive is observed to diminish. This is caused by the exclusion of rays of lower energy.

On the other hand, as the point of observation approaches the magnetic North Pole, it is expected the rate of the arrival of the primary cosmic rays might continue to increase with increasing latitude—unless there exists a solar magnetic field which interferes.

Diamant Manufacturing Corp. Announces New Photographic Equipment.—Jiffy Lens-Ex is a soft lint-free tissue especially created for all precision optical surfaces. It is packed in 100-sheet booklets in a handy 3 × 5 in. size, priced at 24¢ a booklet.

Jiffy Lens Coat is a superb cleaner for all precision optical surfaces designed especially for cleaning coated lenses. The handy 2-oz. bottle lists for 29¢.

The first of its kind, the Jiffy Brilliant Multi-Purpose Enlarger was created especially to fill the ever growing demand for an enlarging tool that will make evenly illuminated, *brilliant* enlargements from both 8 mm., 16 mm., moving picture films and from the new, popular, miniature cameras using 16 mm. film, as well as from 35 mm. films. Designed for professional ease in handling, the Jiffy Brilliant Multi-Purpose Enlarger, despite its extremely compact size, is a versatile instrument that will make enlargements to any size desired from either positive or negative films in both color and black and white.

Electronic Scale Developed to Weigh Livestock.—An electronic scale for weighing livestock at public markets, permitting greater accuracy and speed

and eliminating nearly all possibility of error or incorrect weights, has been developed under the direction of the Production and Marketing Administration, U. S. Department of Agriculture.

The new scale measures the weight of livestock through electrical impulses and records pressures electrically. When certain buttons are pressed, it prints automatically the weight, number, and type of animals, names of the weigher and selling agency, and the date and time of weighing. It is so constructed that it is impossible to register anything other than the weight of the load actually on the scale platform, and it is accurate to within five pounds on loads up to 32,000 pounds.

The device was developed by an aircraft instrument company, working under contract with the Department under the Research and Marketing Act of 1946. The work was supervised by the Livestock Branch of PMA. The company previously had produced electrical strain-gage cells which are a basic feature of the device and had used them in scales for weighing aircraft. Much modification of the aircraft scale was required to adapt it to use for weighing livestock, and extensive tests and trials at markets were necessary to assure dependability and accuracy under all weather conditions of the changed mechanisms.

Errors of several kinds are possible with the conventional weighbeam type of scale. Dirt accumulations, wear and corrosion tend to reduce accuracy. Dirt and manure on the scale platform are reflected in the weights recorded, unless the scale is frequently rebalanced. Rodents interfering with the weight beam also may cause errors amounting to several hundred pounds. In addition, carelessness or intentional manipulation of the scale by the weigher could produce an erroneous weight record, unless the scale is frequently rebalanced. Weight values indicated on the weighbeam ordinarily can be read only at a very short distance.

With the new scale, the weight is indicated on a large dial, easily readable from ten feet away. Rebalancing of the scale to allow for accumulations on the platform can be accomplished simply by pushing a button.

The electronic scale costs more than conventional scales, but its far greater speed in weighing animals, its higher accuracy, and other points of superiority are believed to more than counterbalance the extra cost. Some stockyard managements already are planning to install scales of this type. The Livestock Branch reports that the new scale undoubtedly will be applicable also to other industries using large-capacity scales.

A detailed report on the scale is being prepared.

New Drug for Parkinson's Disease.—To the thousands who suffer from Parkinson's disease, with its accompanying pathetic palsy and melancholy moods, there's a bright ray of hope for relief through the use of a new drug ARTANE* Trihexyphenidyl Tablets *Lederle* recently developed by Lederle Laboratories Division, American Cyanamid Company at the huge research and manufacturing plant at Pearl River, N. Y.

Without experiencing the side reactions that previous medication for this malady produced, patients taking ARTANE find that the tremors of the

* Reg. U. S. Pat. Off.

hands, the involuntary muscular spasms and the constant drooling are markedly reduced almost immediately after they start taking the tablets.

Furthermore, it has been found that in a high percentage of the cases where ARTANE is used, the mental outlook of the patients is considerably brightened and they are then more easily persuaded to take part in activities that may have additional therapeutic effects.

Physicians who have given ARTANE in clinical trials agree that it is the best palliative for Parkinson's disease that is available at the present time. In addition, they consider the new Lederle drug remarkable in that it is effective about 90% of the time against a condition as severe as Parkinsonism and in cases where heretofore the patients have had constant treatment for many years with little success. ARTANE is now available throughout the country for physicians to prescribe.

The tablets come in two sizes, 2 milligram and 5 milligram, and Lederle packages both in bottles of 100 and 1,000 ARTANE tablets.

New Film Illustrates on-the-Job Fabricating and Erecting Techniques for Low-Cost Trussed Rafter.—Builders of multi-unit dwelling projects now have an opportunity to follow, through motion pictures, actual on-the-job truss fabricating techniques which are permitting builders to reduce roof framing material and labor as much as 25 per cent.

The Timber Engineering Company, Washington, D. C., has just announced the availability, for free use by architectural and building groups, of a 16-mm. motion picture covering the mass manufacture and assembly of 3,500 timber connector equipped trussed rafters used in the Bonhaven Apartments, Richmond, Va. The picture is a single reel, black and white silent film which requires 18 minutes for projection.

V.2
194

The new film depicts in detail the quantity production methods used to fabricate, assemble and erect the new low-cost trussed rafter which has been used in over 17,000 housing units in the last three years. The rafter itself is a simple, four-member assembly composed of standard 2×4 and 2×6 lumber. It is designed to cover spans up to 32 feet.

The member sizes in the trussed rafter are small because the Teco Timber Connectors in the joints permit use of the full allowable working stress for the members.

Because of their extreme simplicity and economy of material, the trusses have been fabricated and erected in quantity at costs as low as $9.89 each in place. The basic design, which is available in four pitches, requires no left or right hand members and makes turning of the truss during assembly unnecessary.

Distribution of the film is being handled directly by the Timber Engineering Company. Copies may be secured by interested groups by writing the company at 1319-18th Street, N. W., Washington, D. C.